Infinite Levels of Complexity in a Family of One-Dimensional Singular Dynamical Systems

Evan Oman

Advisor: Bruce Peckham

August 25, 2015

University of Minnesota Duluth

CONTENTS

1. INTRODUCTION

A broad spectrum of Discrete Dynamical Systems research has been dedicated to understanding rational maps of the plane such that $f : \mathbb{R}^2 \to \mathbb{R}^2$. The goal of any such study is to develop a description of the "full dynamics" of the chosen family of maps as stated below:

Full Dynamics of a Family of Maps

The full dynamics of some family of maps $f_{\alpha_1,\alpha_2,\ldots,\alpha_i} : S \to S$ is the characterization of the long term behavior of every point $s \in S$ under f as the parameters α_i vary.

One special family of maps of $\mathbb{R}^2$, defined in complex coordinates, is the quadratic family defined as follows:

$$z_n \mapsto Q_c(z_n) = z_n^2 + c = z_{n+1} \tag{1.1}$$

where $z \in \mathbb{C}$. This family has been been studied extensively in both the one and two dimensional settings [3]. We will explore a singular perturbation of this well known family by adding an inverse square conjugate term with perturbation parameter β which yields the system:

$$z_n \mapsto f_{c,\beta}(z_n) = z_n^2 + c + \frac{\beta}{\overline{z}_n^2} = z_{n+1} \tag{1.2}$$

Robert Devaney and others have studied very similar maps, in particular Devaney et al. consider the map $z^2 + c + \frac{\lambda}{z^2}$ in [4]. The family listed in Eq. 1.2 differs by adding a complex conjugate term, making the perturbation not only singular but also nonholomorphic (since it is well know that any map containing $\overline{z}$ cannot be holomorphic). The goal of this study is to compare the well known dynamics of the standard quadratic family with the dynamics of our perturbed family in order to illuminate how the two families differ. We will begin with a summary of some results, definitions, and theorems from the field of Dynamical Systems. Next we present some one-dimensional results showing that the singularity introduces an infinity of significant parameter values, some corresponding to superattracting periodic orbits and others to parameter values for which the critical point maps to ∞ within a finite number of iterates. Finally, we conclude by briefly discussing how the one-dimensional results relate to the larger two-dimensional system.

2. BACKGROUND FROM DYNAMICAL SYSTEMS

This chapter will introduce some of the basic ideas from the study of Dynamical Systems. We begin with a more formal definition of the "long-term behavior" of points in the domain by introducing the orbit of a point. Note that for the remainder of this chapter we assume that our family is defined by $f_{\alpha_1,\alpha_2,\ldots,\alpha_n} : S \to S$ where α_i is a parameter of the map f.

Definition 2.1: Forward Orbit of a Discrete System[2]

The forward orbit of some $x \in S$ is the set of points $x, f(x), f^2(x), \ldots$ and is denoted by $O^+(x)$. If f is a homeomorphism, we may define the full orbit of x, $O(x)$, as the set of points $f^n(x)$ for $n \in \mathbb{Z}$, and the backward orbit of x, $O^-(x)$, as the set of points $x, f^{-1}(x), f^{-2}(x), \ldots$.

Note that when f is not a homeomorphism, there is no unique backward orbit. However, one may refer a backward orbit specifically by choosing particular preimages at each backward iterate. Thus when we say we want to understand the longterm behavior for every point in the domain, we mean that we want to be able to characterize the set $O^+(x)$ for every $x \in S$ as our parameters vary. A useful dichotomy that is often introduced is to divide the domain into points whose orbits stay bounded and those points whose orbits do not stay bounded. An orbit is said to escape (become unbounded) when successive iterates can grow arbitrarily large and then increase indefinitely without bound. For many maps, such as the $f_{c,\beta}$ map which we will explore in this paper, escape criteria exist to determine a radius beyond which future iterates will only increase without bound[1]. Alternatively, the orbit of a point x stays bounded when, regardless of the number of iterates, the points in the set $O(x)$ remain within some ball with finite radius. There are several situations where this can occur, we define a few of the more important cases below.

Definition 2.2: Fixed and Periodic Orbits[2]

The point x is a fixed point for f if $f(x) = x$. The point x is a periodic point of period n if $f^n(x) = x$. The least positive n such that $f^n(x) = x$ is called the prime period of x. The set of points in the orbit of a periodic point form a periodic orbit. Eventually fixed points have an identical definition with $n = 0$.

Thus if a point x is fixed or periodic, then $O^+(x)$ will remain bounded under repeated iteration. In addition to being fixed or periodic, points can also be eventually fixed/periodic.

Definition 2.3: Eventually Fixed/Periodic Points[3]

A point x is eventually periodic of period n if x is not periodic but there exists $m > 0$ such that $f^{n+i}(x) = f^i(x)$ for all $i \geq m$. That is, $f^i(x)$ is periodic for $i \geq m$.

Additionally, points may be asymptotically attracted to a point if that point is attracting. Alternatively orbits may be pushed away from a point if it is repelling. The following definition determines when each of these behaviors may occur:

Definition 2.4: Attracting and Repelling Fixed Points[3]

Suppose x is a fixed point for f where f is a one-dimensional map. Then x is an attracting fixed point if $|f'(x)| < 1$. The point x is a repelling fixed point if $|f'(x)| > 1$. Finally, if $|f'(x)| = 1$, the fixed point is called linearly neutral or indifferent.

Thus even if a point is not itself along a fixed or periodic orbit, it can still stay bounded by being drawn into an attracting periodic point. We say that these points are asymptotically fixed because they limit to the attracting point but do not reach that point in finite time. Additionally, points may stay bounded even if they are never drawn toward an attracting periodic orbit, such as in the case of certain chaotic maps where the orbits of some special points remain bounded forever, never hitting the same point twice while densely filling a region of phase space.

In addition to points which correspond to bounded orbits, the critical points of a system play a key role due to the fact that they have slope 0 (in one dimension), making them "superattracting". Chapter 3 will make heavy use of critical points and will further discuss their significance.

Definition 2.5: Critical Point [2]

A point x is a critical point of a one-dimensional map f if $f'(x) = 0$ or if $f'(x)$ does not exist. The critical point is degenerate if $f''(x) = 0$ or does not exist and non-degenerate otherwise.

Now that we have introduced some of the main terminology, we will discuss some of the numerical/visual techniques that are used to develop an overview of the behavior of a system. We will begin with a simple tool for one-dimensional dynamics called graphical iteration. This technique is simply the process of graphically representing the orbit of some point in the x_n vs x_{n+1} space. First we graph $x_{n+1} = f(x_n)$ and the reference line $x_{n+1} = x_n$. For some seed value x_0, we start at the point (x_0, x_0) and then draw a vertical line from (x_0, x_0) to our curve in (x_n, x_{n+1}) space, giving us the point $(x_0, f(x_0)) = (x_0, x_1)$. We go then back to the reference line at (x_1, x_1), completing our first iterate. Continuing in this manner we arrive at a series of lines "to the graph and over" which show the orbit of x_0 as it moves from iterate to iterate. Figure 2.1 shows several such iterations on the graph of $x^2 - 0.1$, showing how the orbit of $x_0 = 1$

is attracted to the left hand fixed point.

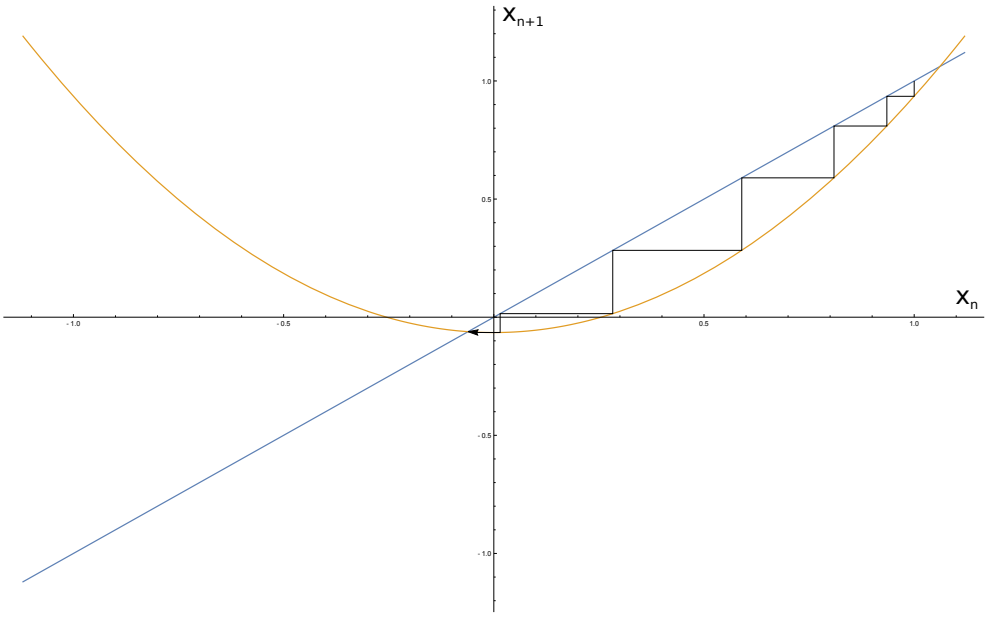

Fig. 2.1: Graphical Iteration on $x^2 - 0.1$ with $x_0 = 1$

A different picture that is often used for the study of a one dimensional dynamical system is an Orbit Diagram. An Orbit Diagram is a picture in parameter×phase space created by sampling a range of parameter values, computing the first n iterates of some seed value, and then plotting the last m of those n points. The images shown in Figures 3.1 and 3.2 were made by plotting the 400^{th} through 500^{th} iterates for 20,000 uniformly sampled parameter values. The reason why these images are useful is because they roughly show how long term behaviors are changing as the chosen parameter varies: by 400 to 500 iterates most points have either escaped or fallen into some bounded pattern, thus giving an approximation of long term behavior. Typically critical points are chosen as the seed value for such a plot; again we will discuss the reasons for this choice in Chapter 3.

A final numerical technique which is useful for maps of the plane is the creation of escape pictures which quickly express the escape rates for different seed values in the plane. Typically we use two types of escape pictures: one which is in phase space and the other which is in parameter space. Phase space pictures fix all parameters and take each "pixel" as an initial condition in the plane to be iterated. The pixel for each point is then colored according to the relative amount of time that is takes to escape (where escape is typically determined by some iterate landing outside a ball of some predetermined radius). Similarly, a parameter space image takes each pixel as a parameter value and then iterates a critical point, recording escape in a similar manner to the phase space images. Figure 2.2 shows two parameter space escape images and two phase space escape images for the quadratic and perturbed maps.

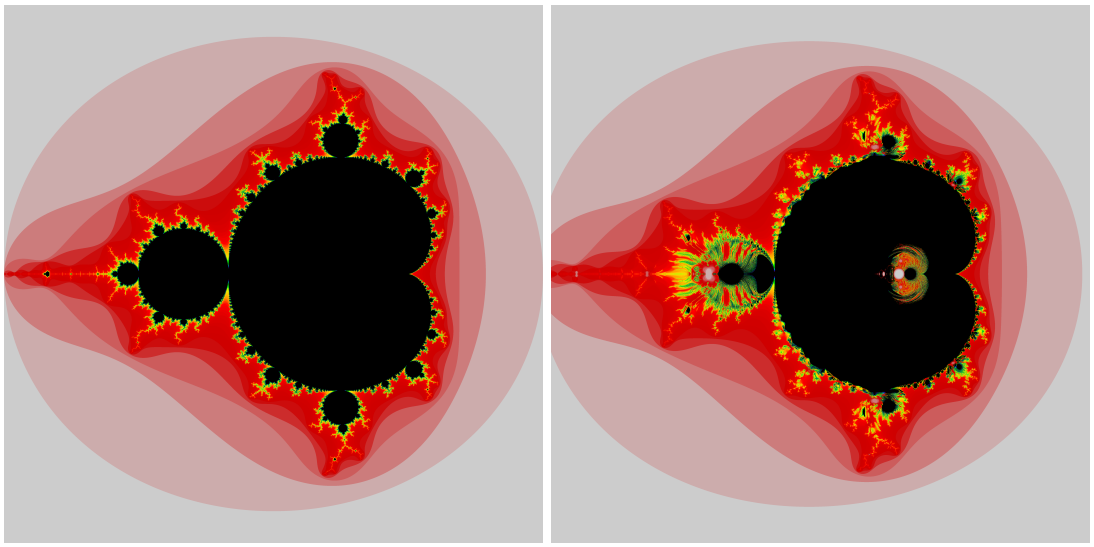

(a) Parameter Space Escape image for $z^2 + c$ (Mandelbrot set)

(b) Parameter Space Escape image for $z^2 + c + \frac{.001}{z^2}$

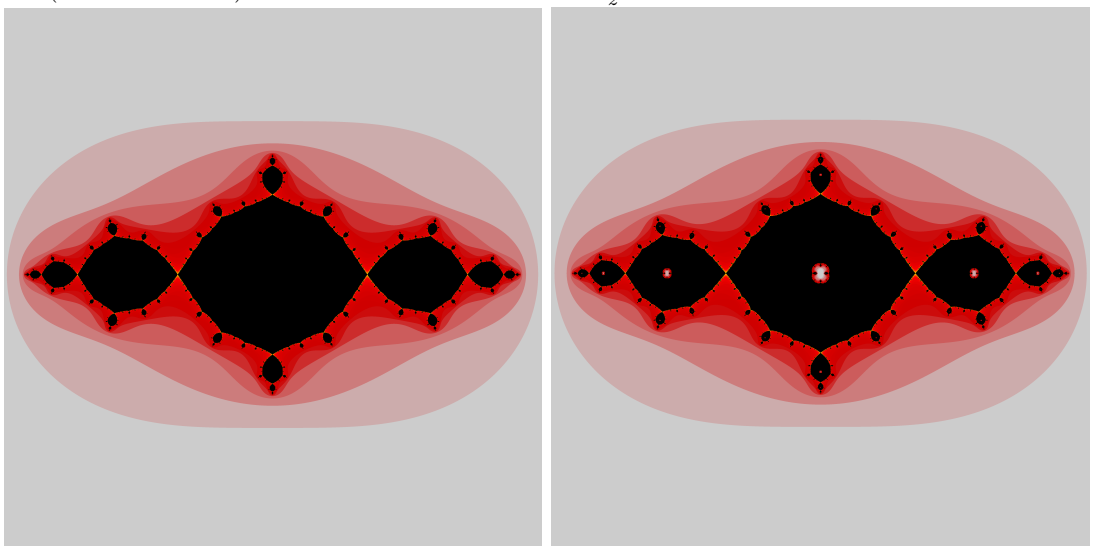

(c) Phase Space Escape image for $z^2 - 1$

(d) Phase Space Escape image for $z^2 - 1 + \frac{.001}{z^2}$

Fig. 2.2: Escape diagrams for the quadratic and perturbed families

3. OVERVIEW OF ONE DIMENSIONAL RESULTS

In this chapter we will give an overview of results pertaining to the one-dimensional family $f_{c,\beta}(x) = x^2 + c + \frac{\beta}{x^2}$ where $x, c, \beta \in \mathbb{R}$. Furthermore, we will fix the parameter β at .001 and consider the structure of the resulting system $f_c(x) = x^2 + c + \frac{.001}{x^2}$ as the parameter c is varied. Comparisons will be drawn

against the standard quadratic map $Q_c(x) = x^2 + c$ and the results which are proven in the next chapter will be introduced and discussed.

3.1 Preliminary Numerical Experiments

When first considering some dynamical system, the critical points tend to be a focus of preliminary attention because they play an important role in the overall dynamics of the system. To see why, we introduce the Schwarzian Derivative and a theorem which tells us how the critical orbit can help determine the behavior of all other orbits.

Definition 3.1: Schwarzian Derivative[3]

The Schwarzian Derivative of a function F is given by:

$$SF(x) = \frac{F'''(x)}{F'(x)} - \frac{3}{2}\left(\frac{F''(x)}{F'(x)}\right)^2$$

Theorem 3.1:

Suppose $SF(x) < 0\ \forall x$ where SF is the Schwarzian Derivative of some function F. Then, if x_0 is an attracting periodic point for F, either the immediate basin of attraction of x_0 extends to $+\infty$ or $-\infty$, or else there is a critical point of F whose orbit is attracted to the orbit of x_0[3].

For our family, as a rational map of $\mathbb{R}$, infinity is attracting so no attracting periodic orbit can have a basin of attraction which extends to $\pm\infty$. Thus if an attracting periodic orbit exists in a system such as ours, which also has a negative Schwarzian Derivative, then the orbit of the some critical point will be attracted towards that periodic orbit. The main restriction of this theorem is that F must have a negative Schwarzian Derivative, a requirement that our function satisfies as we see below.

Proposition 3.1:

The function $f_{c,\beta}(x) = x^2 + c + \dfrac{\beta}{x^2}$ has a negative Schwarzian Derivative for $\beta \geq 0$.

Proof:

Computing the Schwarzian Derivative of our function $f_{c,\beta}$ we see that

$$Sf_{c,\beta}(x) = \frac{\frac{\partial^3}{\partial x}\left(x^2 + c + \frac{\beta}{x^2}\right)}{\frac{\partial}{\partial x}\left(x^2 + c + \frac{\beta}{x^2}\right)} - \frac{3}{2}\left(\frac{\frac{\partial^2}{\partial x}\left(x^2 + c + \frac{\beta}{x^2}\right)}{\frac{\partial}{\partial x}\left(x^2 + c + \frac{\beta}{x^2}\right)}\right)^2 = -\left(\frac{24\beta x^2}{(\beta - x^4)^2} + \frac{3}{2x^2}\right)$$

Thus, if β is positive or zero, each term inside the parentheses is positive because every x is raised to an even power. Therefore we have the negation of a strictly positive term so we can conclude that $\forall x$,

$Sf_{c,\beta}(x) < 0$. □

Therefore our function has a negative Schwarzian Derivative for $\beta \geq 0$ so an analysis of the critical orbit(s) should provide a classification of all attracting periodic points in the system. The critical points of our system are given by solving for the roots of our derivative:

$$\frac{\partial f_{c,\beta}(x)}{\partial x} = 0 \Rightarrow 2x - \frac{2\beta}{x^3} = 0 \Rightarrow 2x = \frac{2\beta}{x^3} \Rightarrow x = \pm\beta^{\frac{1}{4}}$$

Thus we have two critical points in the real setting. However, when we plug these points into $f_{c,\beta}$ we see that:

$$f_{c,\beta}(\beta^{\frac{1}{4}}) = \left(\beta^{\frac{1}{4}}\right)^2 + c + \frac{\beta}{\left(\beta^{\frac{1}{4}}\right)^2} = 2\beta^{\frac{1}{2}} + c = \left(-\beta^{\frac{1}{4}}\right)^2 + c + \frac{\beta}{\left(-\beta^{\frac{1}{4}}\right)^2} = f_{c,\beta}(-\beta^{\frac{1}{4}})$$

Therefore, while we have two critical points, we really only have one critical value which implies that the orbits of $\pm\beta^{\frac{1}{4}}$ are identical after the first iterate.

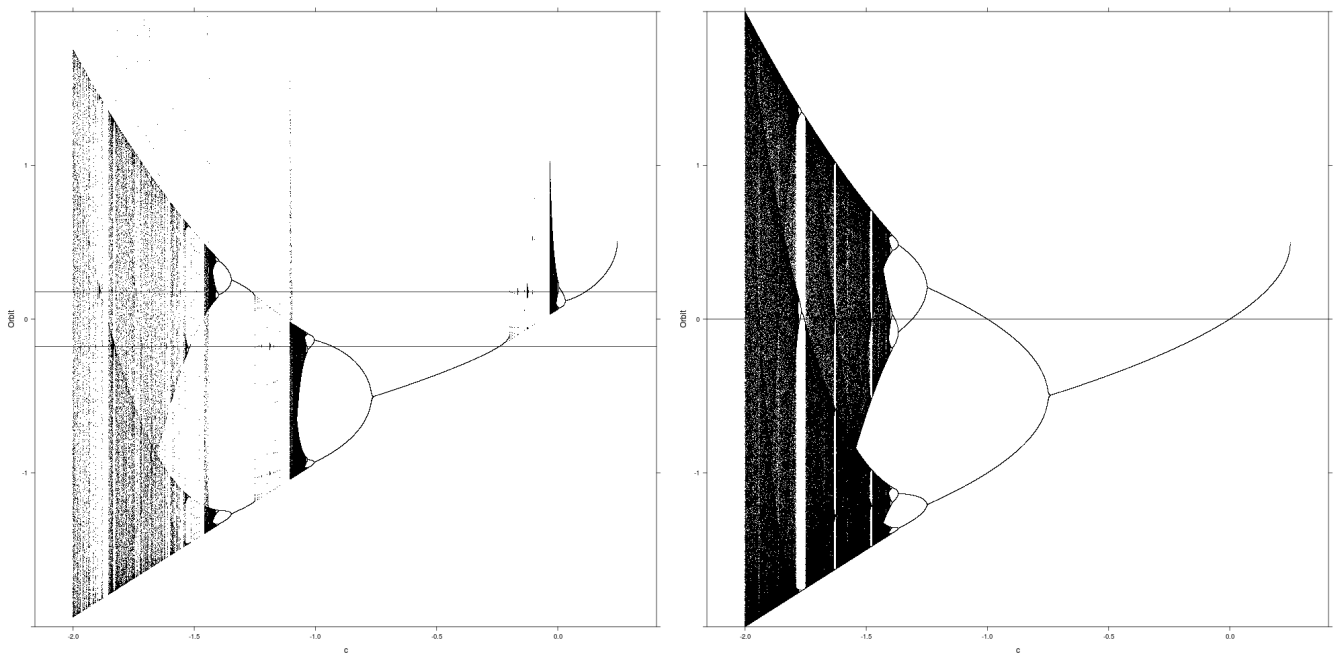

(a) Orbit diagram of $x^2 + c + \frac{.001}{x^2}$ *(b)* Orbit diagram of $x^2 + c$

Fig. 3.1: Orbit diagrams of the perturbed system and the original system

Now that we have established that the behavior of the critical orbit helps determine the behavior of the system, we can perform a few numerical experiments to discover where the dynamics of the perturbed system varies from the dynamics of the original quadratic map $Q_c(x) = x^2 + c$. As previously discussed, a standard analysis of the behavior of the critical orbit is to create an orbit diagram as shown in Figure 3.1a

and Figure 3.1b. Immediately we can see some major differences between the behavior of the two families. One of the most notable differences is on the parameter interval $c \in (-.25, .05)$ (magnifications of which are shown in Figures 3.2a and 3.2b).

The following section will discuss the behavior of the system for c intervals which are either straightforward or analogous to the behavior of the original quadratic map. Subsequent sections will then describe some of the behavior where the perturbed map acts quite differently than the standard map, providing some instances of interesting critical orbit behavior. Since $\beta = .001$ is fixed from this point forward, we will refer to $f_{c,\beta=.001}$ as f_c.

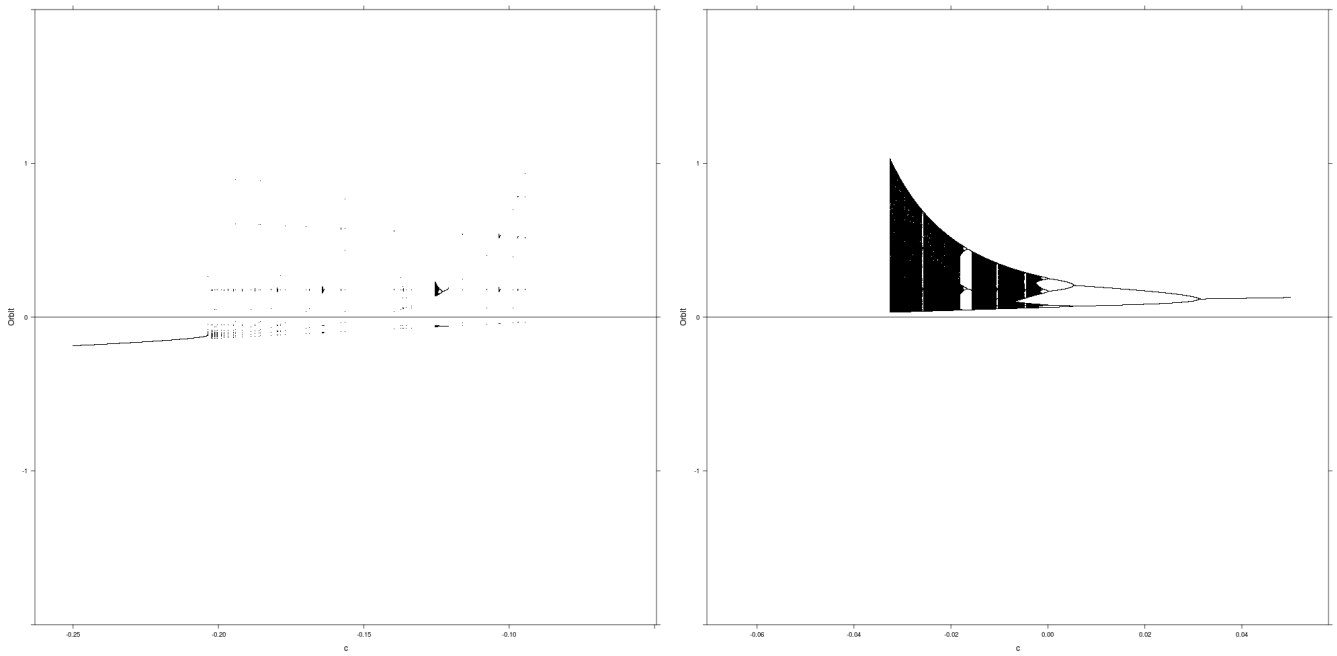

(a) $c \in (-.25, -.062456)$ *(b)* $c \in (-.062456, .05)$

Fig. 3.2: Zooms of the perturbed system's orbit diagram

3.2 Intervals of Understood Behavior

A cursory review of the orbit diagrams in Figure 3.1 reveals that the overall behavior of the systems seems to be quite similar, with many regions being nearly identical while some are entirely different. This section will focus on the former type of parameter intervals, briefly covering regions were the dynamics are fairly straightforward/similar to well known behaviors. In addition to the numerical bounds for each interval, we will include the special parameter names with orbit codings which will be introduced in the next section. Note that Figure 3.10 provides graphical iteration of the positive critical point for most of the parameter values described below. These images may prove useful when trying to visualize how the system is changing

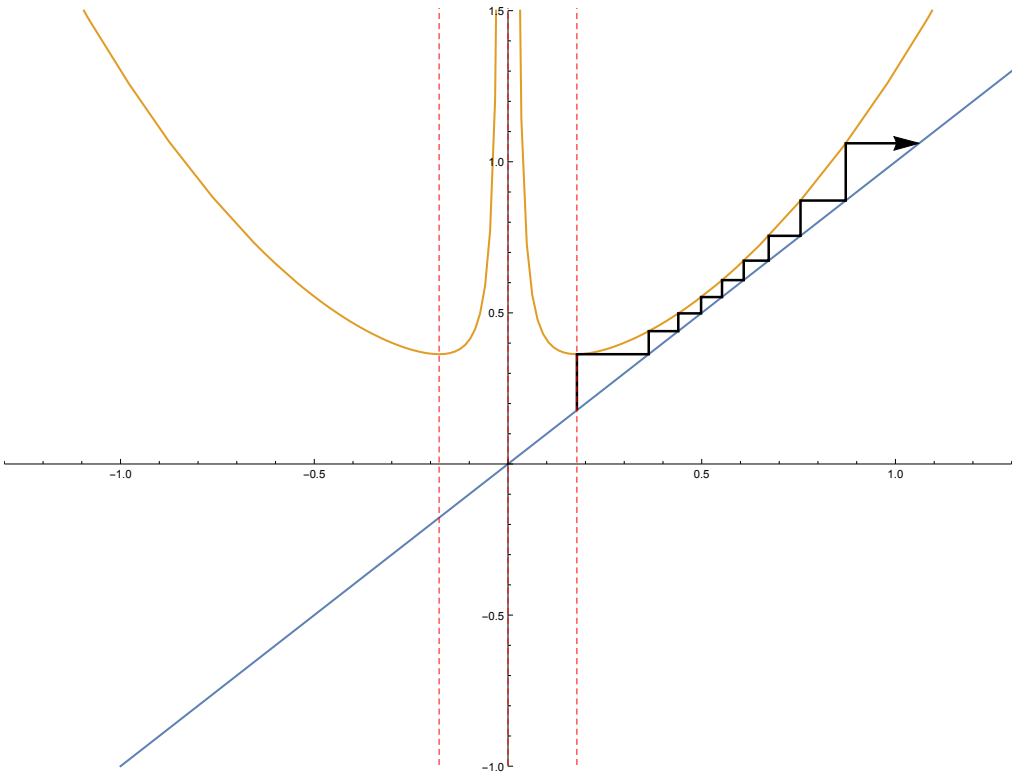

Fig. 3.3: Graphical iteration of the positive critical point under $x^2 + .3 + \frac{.001}{x^2}$, showing escape

at each parameter value.

$\underline{c > .24604 \approx s_1^r}$

For $c > .24604$, $f_c(x)$ behaves in a very similar manner to $Q_c(x)$ for $c > .25$ in that the plot is entirely above the reference line, as shown in Figure 3.3. In both cases, all orbits escape because the function has no fixed points or periodic behavior so there is nothing to prevent all orbits from escaping to ∞ (hence the white space in our orbit diagrams). This interval of universal escape ends when the $f_c(x)$ undergoes a saddle node bifurcation at $c \approx .24604 \approx s_1^r$. This change is analogous to the saddle node of $Q_c(x)$ which occurs at $c = .25$.

$\underline{c \in (-.03255, .24604) \approx (h_2^{CLP_c}, s_1^r)}$

Following the saddle node bifurcation and until $c \approx -.035$, the perturbed system seems to be going through the standard period doubling route to chaos that is similar to the behavior exhibited by $Q_c(x)$ for $c \in (-2, .25)$. Figure 3.4 shows a zoom of the perturbed map over $c \in (-.35, .05)$ along side the orbit diagram for $Q_c(x)$. While the exact shapes of the two images are slightly different, it is readily apparent that the two systems are exhibiting nearly identical behavior, that is to say that they appear to be topologically equivalent. For example, we can trace out the sequence of period doublings from 1 to 2 to 4 and so on, as well as match other windows (especially the period three which is very clear on

both diagrams). The reason for this similarity is that on this parameter interval, the bimodal map $f_c(x)$ is actually acting as a unimodal map because the entire curve is above 0, meaning that all orbits are acting on only the right portion of the curve after at most one iterate. Additionally, this unimodal map has a very similar shape to that of the quadratic map, causing a similar sequence of bifurcations to occur. Thus this interval has been reduced to already known results and we expect that the methods from the study of the $Q_c(x)$ map would be able to describe the behavior observed over this parameter interval.

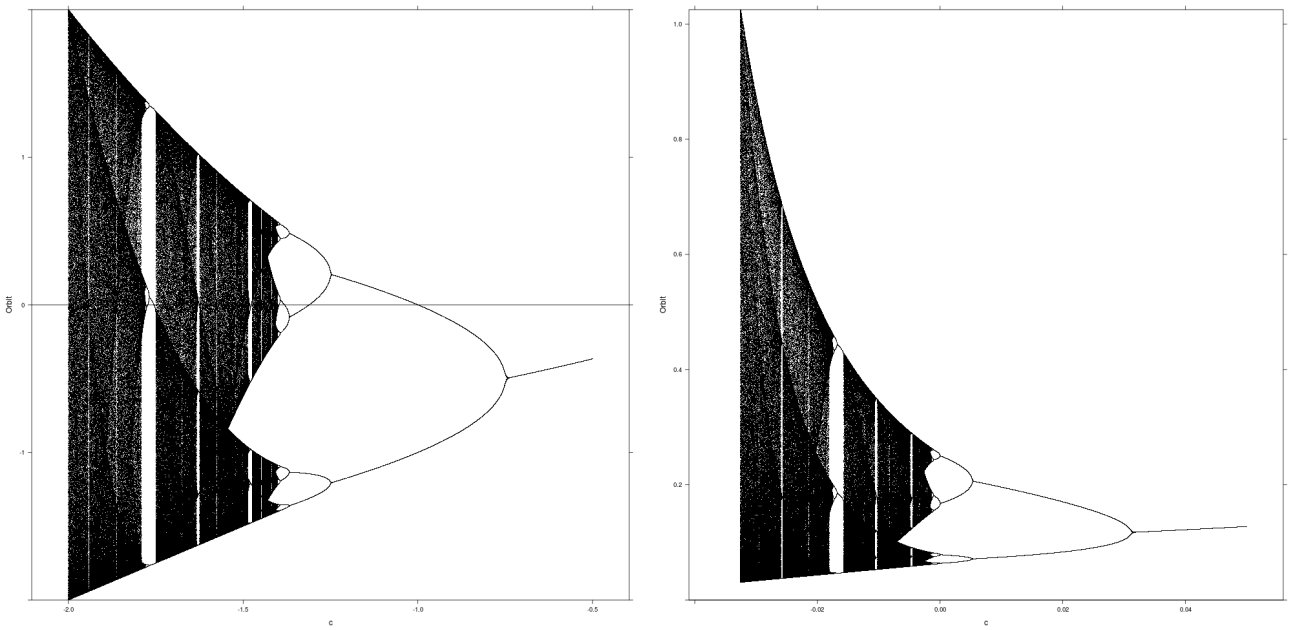

(a) Orbit Diagram for $Q_c(x)$ where $c \in (-2, -.5)$ *(b)* Orbit Diagram for $f_c(x)$ where $c \in (-.035, .05)$

Fig. 3.4: Orbit diagrams of the original system and the perturbed system

$\underline{c \in (-.0632456, -.03255) \approx (z_1^{C0}, h_2^{CLP_c})}$

For $c < -.03255$, the critical value first escapes by mapping just to the right of the right hand fixed point and then continuing to infinity. Thus the dynamics on this interval would be very similar to the dynamics of $Q_c(x)$ for $c < -2$ where the critical orbit escapes leaving a Cantor set of points which stay bounded. Again similar techniques from the quadratic map study would likely be able to prove that the dynamics on this remaining Cantor set would exhibit chaotic behavior when considered under a conjugacy with the Shift Map on two symbols. As c continues to drop, this first iterate of the critical value is mapped higher and higher up the singularity around 0 until $c \approx -.0632456 \approx z_1^{C0}$ where $f_c(C) = 0$ as we see below:

$$f_c(C) = 0 \Rightarrow \left(\beta^{\frac{1}{4}}\right)^2 + c + \frac{\beta}{\left(\beta^{\frac{1}{4}}\right)^2} = 0 \Rightarrow c = -2\beta^{\frac{1}{2}} \Rightarrow c = -2(.001)^{\frac{1}{2}} \Rightarrow c \approx -.0632456 \approx z_1^{C0}$$

Thus at the parameter value z_1^{C0} the n^{th} iterate of the critical point maps directly to ∞ for $n > 1$.

$c \in (-.092495, -.0632456) \approx (h_2^{CLP_c}, z_1^{C0})$

As c decreases from z_1^{C0}, the second iterate of the critical point moves down the left side of the singularity until the parameter value $c \approx -.092495$ which is the point where the first iterate is small enough such that the second iterate is exactly the right hand fixed point P_c. Once the second iterate lands below P_c, the behavior is no longer similar to the behavior of $Q_c(x)$ for $c < -2$. Again refer to Figure 3.10 for graphical iteration depicting most of the changes discussed here

$c \in (-.241073, -.092495) \approx (p_1^{-C}, h_2^{CrP_c})$

This interval is the subject of the following sections where it will be described in detail.

$c \in (-2.1, -.241073) \approx (h_2^{ClP_c}, p_1^{-C})$

In this interval, f_c again acts in a similar manner to the $Q_c(x)$ map because whenever the critical orbit stays far enough away from the singularity, the global geometry of the curve has more influence than the singularity. However we do note several significant deviations from the $Q_c(x)$ dynamics, most notably where the map "should" undergo a period doubling bifurcation. Instead, the $f_c(x)$ orbit diagram seems to be filling an interval of orbit values, indicating more complicated behavior. Additionally, the orbit diagram isn't nearly as well filled in at other points (even though the same number of iterates were plotted in either case). This is likely due to the many complicated ways by which points may escape through the "trap door" near $x = 0$. Further study would be required to fully understand the behavior on this interval and appreciate its similarity/dissimilarity to $Q_c(x)$.

$c < -2.1 \approx h_2^{ClP_c}$

On this interval, the critical orbit again escapes because its second iterate lands to the right of the right hand fixed point P_c. Again the dynamics on this interval would be similar to that of the $Q_c(x)$ map for $c < -2$ where there would be a Cantor set of points remaining. Here though, instead of two preimages of every escaping interval as we have with $Q_c(x)$, $f_c(x)$ would have four preimages of the escaping interval due to its bimodal shape. Thus instead of the middle thirds Cantor set for $Q_c(x)$, we would likely have a middle "four ninths" Cantor set of points which do not escape. The dynamics of the points in this set should be conjugate to the shift map on four symbols.

3.3 Orbit Codings

Before introducing our results, we will discuss one final analytical technique which is critical to understanding the results presented in the following sections. It is common in the study of one-dimensional

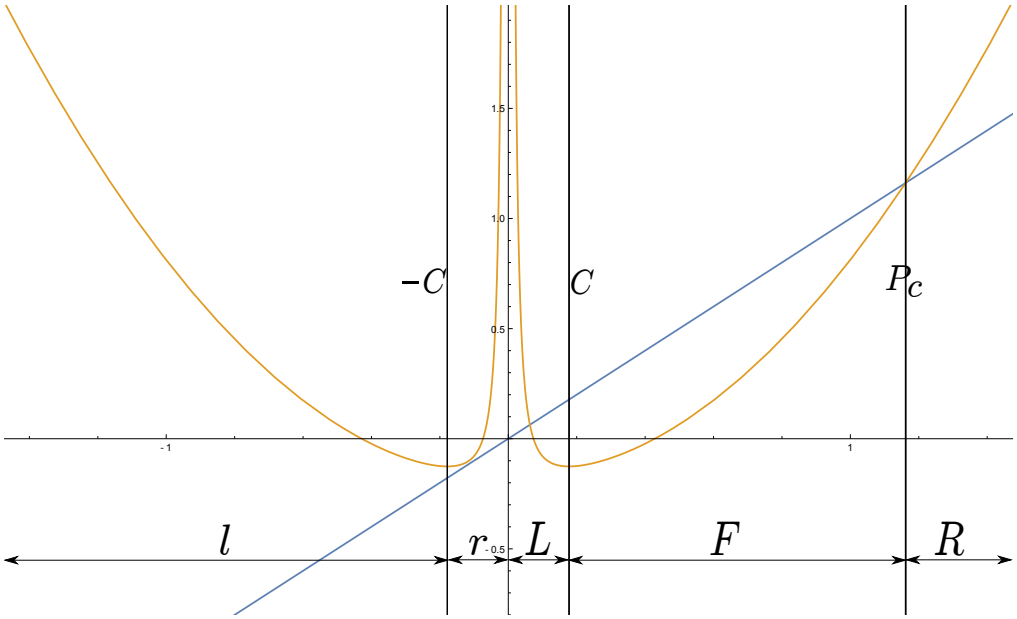

Fig. 3.5: A partitioning of the domain of the map $f_c(c) = x^2 + c + \frac{.001}{x^2}$

dynamical systems to partition the the domain/codomain into a series of intervals. Once such a partition has been established, we can then encode orbits with a sequence of symbols determined by which partition each iterate maps to. The reason why this is useful is because we can look at the coding of a some orbit, say the critical orbit, and keep track of changes in that coding as the parameter set changes. Typically when such a coding change occurs, the system has undergone some kind of shift as we moved from one parameter value to another. Therefore, orbit codings provide a simple numerical mechanism for detecting behavioral transitions. For parameter values within our interval of interest, we will impose the following partitioning for our system:

- Let C be the positive critical point such that $C = +\beta^{\frac{1}{4}} = .001^{.25} \approx 0.177827$. $-C$ will simply denote the negative critical point.
- Let P_c be the right most fixed point (when it exists) which is given by solving for the maximum c value which satisfies $f_c(x) = x$. The curve in c space produced by the solution of this system is shown in Figure 3.6.
- R: Corresponds to $\{x | x \in (P_c, \infty)\}$. Over this interval, $f_c(x)$ is always increasing with respect to x for all c. Additionally, once any iterate lands in this interval escape is inevitable.
- F: Corresponds to $\{x | x \in (C, P_c)\}$. Over this interval, $f_c(x)$ is increasing with respect to x for all c.
- L: Corresponds to $\{x | x \in (0, C)\}$. Over this interval, $f_c(x)$ is decreasing with respect to x for all c.

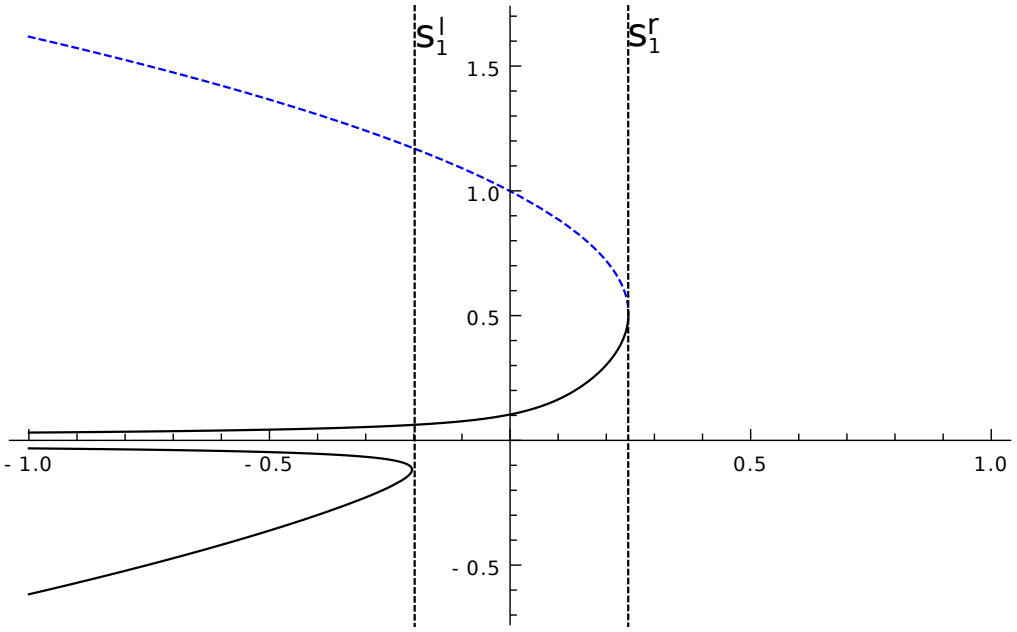

Fig. 3.6: Plot of all the fixed points with respect to c, P_c is the max such value for any c (shown in a dashed line)

- r: Corresponds to $\{x|x \in (-C, 0)\}$. Over this interval, $f_c(x)$ is increasing with respect to x for all c.
- l: Corresponds to $\{x|x \in (-\infty, -C)\}$. Over this interval, $f_c(x)$ is decreasing with respect to x for all c.
- In addition to the above intervals, we will also define codes corresponding to boundary points: 0, C, $-C$, P_c, and ∞ where C and $-C$ are the critical points of our system and P_c is the rightmost fixed point.

Note that the intervals l, r, and L are invariant under changes in our parameter c (because the critical points are not a function of c) while F and R are dependent on the value of P_c which depends on c. See Figure 3.5 for a graphical representation of these intervals. Throughout the remainder of this paper, we will make heavy use of critical orbit codings of the form $C\alpha_1\alpha_2\cdots\alpha_n$. As mentioned above, keeping track of such codings is useful because they can easily detect when some i^{th} iterate moves from one interval to another. This is significant not only because it could mark the difference between bounded and unbounded orbits, but because between any two distinct codings, there are the significant values $-C$, 0, C, and P_c. Thus, since our map varies continuously with respect to both c and x (see Proposition 4.1), if α_i changes from one coding at the value c_1 to another coding at c_2, we are guaranteed by the Intermediate Value Theorem that the i^{th} iterate must have taken on an intermediate value according to Table 3.1 (note that all transitions are transitive such that a transition $l \to L$ implies $l \to r$ and $r \to L$).

Coding Transition	Guaranteed Intermediate Value
$l \leftrightarrow r$	$-C$
$r \leftrightarrow L$	0
$L \leftrightarrow F$	C
$F \leftrightarrow R$	P_c

Tab. 3.1: Summary of coding transitions and their implications

3.4 Parameter Interval of Interest and Naming Conventions

The goal of subsequent sections is to introduce the results concerning the behavior of the critical orbits of f_c within the parameter interval $(-.25, -.062456)$ as discussed in Section 3.2. Before doing so, we will briefly introduce some naming conventions which will aid our description of the behavior in this interval: In addition to the codes defined in Section 3.3, we will adopt the following naming conventions for simplicity:

- Let $\text{int}\{a, b\} = (\min\{a, b\}, \max\{a, b\})$ such that $\text{int}\{a, b\}$ is simply the interval between a and b where $a > b$ or $b > a$.

- Let h_n, p_n, z_n be parameter values such that $f_{h_n}^n(C) = P_c$ (corresponding to a homoclinic parameter value), $f_{p_n}^n(C) = C$ (corresponding to a superattracting periodic orbit parameter value), and $f_{z_n}^n(C) = 0$ (corresponding to a prezero parameter value, see Section 4.3). Note that the solutions to these equations are typically not unique; thus we will refer to a specific parameter value with the coding of the critical orbit at that point by placing the coding at that parameter value in the superscript. For example, in Figure 3.7a we see graphical iteration of the critical point at the parameter value $h_2^{CrP_c}$ where we refer to the specific h_2 by listing the coding CrP_c.

- Let s_n be a parameter value where the n^{th} iterate goes through a saddle node bifurcation. We use an l or an r in the superscript to differentiate between the left lobe saddle and the right lobe saddle respectively. s_1^l and s_1^l are labeled in Figure 3.6.

A study of the orbit diagrams from the previous sections reveals that there are several "key" parameter values on the interval $(-.241073, -.092395)$ which can be used to frame our discussion of the critical point behavior. The first, which we call $h_2^{CrP_c}$, occurs approximately at $-.092395$ and represents the first c-value for which the critical orbit stays bounded as c is decreased from z_1^{C0}. See Figure 3.7a for graphical iteration at this parameter value. Additionally, this also happens to be the parameter value where the critical orbit is prefixed at the right hand fixed point, as the notation suggests. We will also call the right hand fixed point at this parameter value the "primary homoclinic point" for reasons which we will discuss in full in

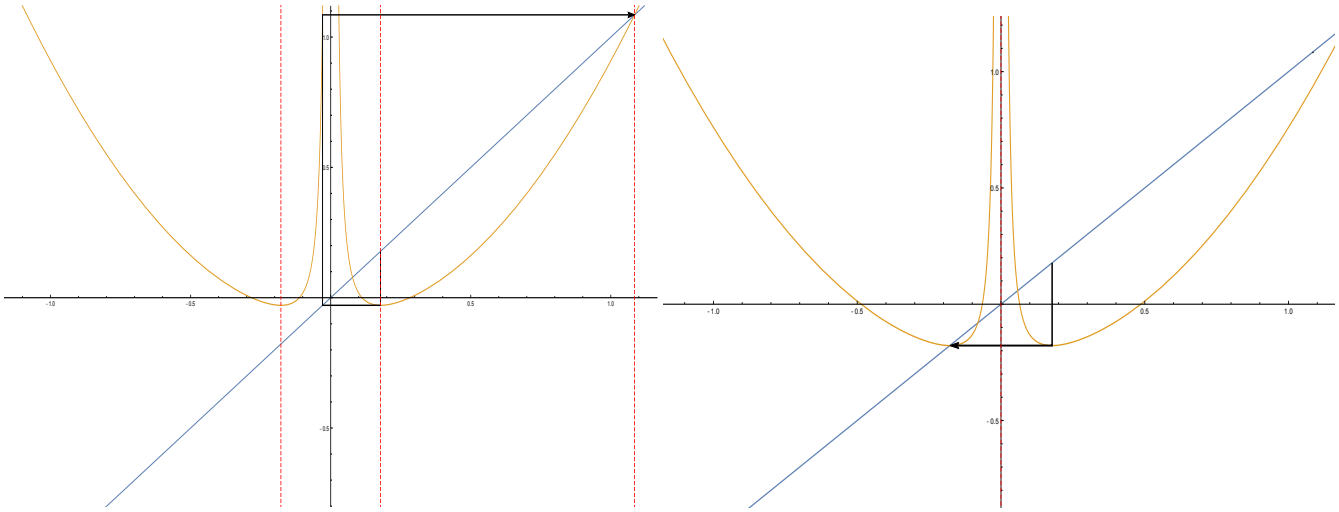

(a) Graphical Iteration of C at the parameter value $h_2^{CrP_c}$ *(b)* Graphical Iteration of C at the parameter value p_1^{-C}

Fig. 3.7: Graphical Iteration at the key parameter values $h_2^{CrP_c}$ and p_1^{-C}

Section 4.1. The second significant parameter value is $p_1^{-C} \approx -.241073$ and represents the point where the negative critical point $-C$ is fixed. See Figure 3.7b for graphical iteration at this parameter value. Note that both of these parameter values yield critical orbits which are fixed after two and one iterates respectively. Thus for any positive integer n, $f^n_{p_1^{-C}}(C) = -C$ and for $n > 1$, $f^n_{h_2^{CrP_c}}(C) = P_c$. This means that higher iterates must be constrained at these points, providing a structure will be exploited in the arguments to follow. Finally, we introduce the point $s_1^l \approx -.203$ which represents the point where the left lobe becomes tangent to the reference line and undergoes a saddle node bifurcation (as the notation suggests). This point is significant because the system seems to return to a behavior more like the original map $Q_c(x)$ for $c < s_1^l$ (as discussed in Section 3.2).

3.5 The Two Primary Accumulation Points

This section will provide a visual overview of the results concerning the two primary sequences of special parameter values as we approach s_1^l from the right and $h_2^{CrP_c}$ from the left. The following propositions from Chapter 4 summarize the accumulation that we are seeing in the figures to follow:

Proposition 4.2: *On the interval $(p_1^{-C}, h_2^{CrP_c})$, there is an accumulation of parameter values p_n and z_n for any integer $n \geq 2$ where the critical orbit has coding $CrF^{n-2}C$ and $CrF^{n-2}0$ respectively. These parameter values have the ordering*

$$z_n < p_n < z_{n+1} < p_{n+1} < \cdots < h_2^{CrP_c}$$

Proposition 4.3: *On the interval* $(p_1^{-C}, h_2^{CrP_c})$*, there is an accumulation of parameter values* p_n*,* z_n*, and* h_n *for any integer* $n \geq 2$ *where the critical orbit has coding* $Cr^{n-1}C$*,* $Cr^{n-1}0$*, and* $Cr^{n-1}P_c$ *respectively. These parameter values have the ordering*

$$p_1^{-C} < \cdots < z_{n+1} < p_{n+1} < h_{n+1} < z_n < p_n < h_n$$

Chapter 4 will introduce the proofs of these propositions; the remainder of this section is devoted to developing some graphical intuition as to how these accumulations propagate. Additionally these figures will serve as a useful reference when reading the proofs of the following chapter. First, Figure 3.8 shows a large zoom of the Orbit Diagram for the parameter interval $(p_1^{-C}, h_2^{CrP_c})$. Labeled on this figure are several of the p_n values described in the above propositions with their coding. Based on a glance of this image, there seems to be some sort of limiting behavior as we approach either side of the parameter interval.

Next, Figure 3.9 shows a plot of $f_c^1(C)$, $f_c^2(C)$, and $f_c^3(C)$ where we are varying our parameter c and looking at how each iterate of the critical point is changing (note that this plot is in the same space as the Orbit Diagram). On this plot we again show the coding intervals and label several of the accumulating parameter values as we approach p_1^{-C} from the right and $h_2^{CrP_c}$ from the left. Hopefully this image provides some sense as to where the special parameter values come from: in this space, they are simply the parameter values of intersections of some iterate of the critical point with some special value 0, C, or P_c, yielding a z_n, p_n, or h_n respectively.

Figures 3.10 and 3.11 provide graphical iteration of the right hand critical point at many of the key parameter values discussed so far. These figures are especially illuminating when considered as a sequence of images as c decreases because one can gain an intuition as to how the system is evolving: as c decreases from $h_2^{CrP_c}$, the second iterate moves down the curve from P_c and in so doing, lands on several points which either cycle back to C (giving a p_n), eventually land on 0 (giving a z_n), or eventually land on P_c (giving an h_n). Again the codings of critical orbit at these parameter values can be constructed by following the graphical iteration.

Figure 3.12 shows a sequence of images which depict the accumulation of p_n and z_n parameter values as we approach $h_2^{CrP_c}$. This sequence of images is a particularly good way to look at the accumulation because it is a visualization of the inductive proof of Proposition 4.2. For any $n \geq 2$, $f_{h_2^{CrP_c}}^n(C) = P_c$ simply because the second iterate is fixed there (fixing all higher iterates). Then as we add higher iterates, we see that $f_{p_n}^{n+1}(C) < 0$, meaning that as the n^{th} iterate makes its way to P_c at $h_2^{CrP_c}$, it must cross the value C, giving a p_n, forcing the next iterate to be negative. In this manner, the proof of Proposition 4.2 constructs

the sequence of p_n and z_n parameter values as required.

In a similar manner to Figure 3.12, Figure 3.13 shows a sequence of images which depict the accumulation of p_n, z_n, and h_n parameter values as we approach p_1^{-C}. Again this is a great visualization of the proof of Proposition 4.3. For any $n \geq 1$, $f^n_{p_1^{-C}}(C) = -C$ simply because the first iterate is fixed there (fixing all higher iterates). Then as we add higher iterates, we see that $f^{n+1}_{z_n}(C) = \infty$, meaning that as the n^{th} iterate makes its way to $-C$ at p_1^{-C}, it must cross the value 0, giving a p_n, h_n, and then finally a z_n, forcing the next iterate to be ∞. This iterate must also make its way down to $-C$ so continuing in this manner, the proof of Proposition 4.3 constructs the sequence of p_n, h_n, and z_n parameter values as required.

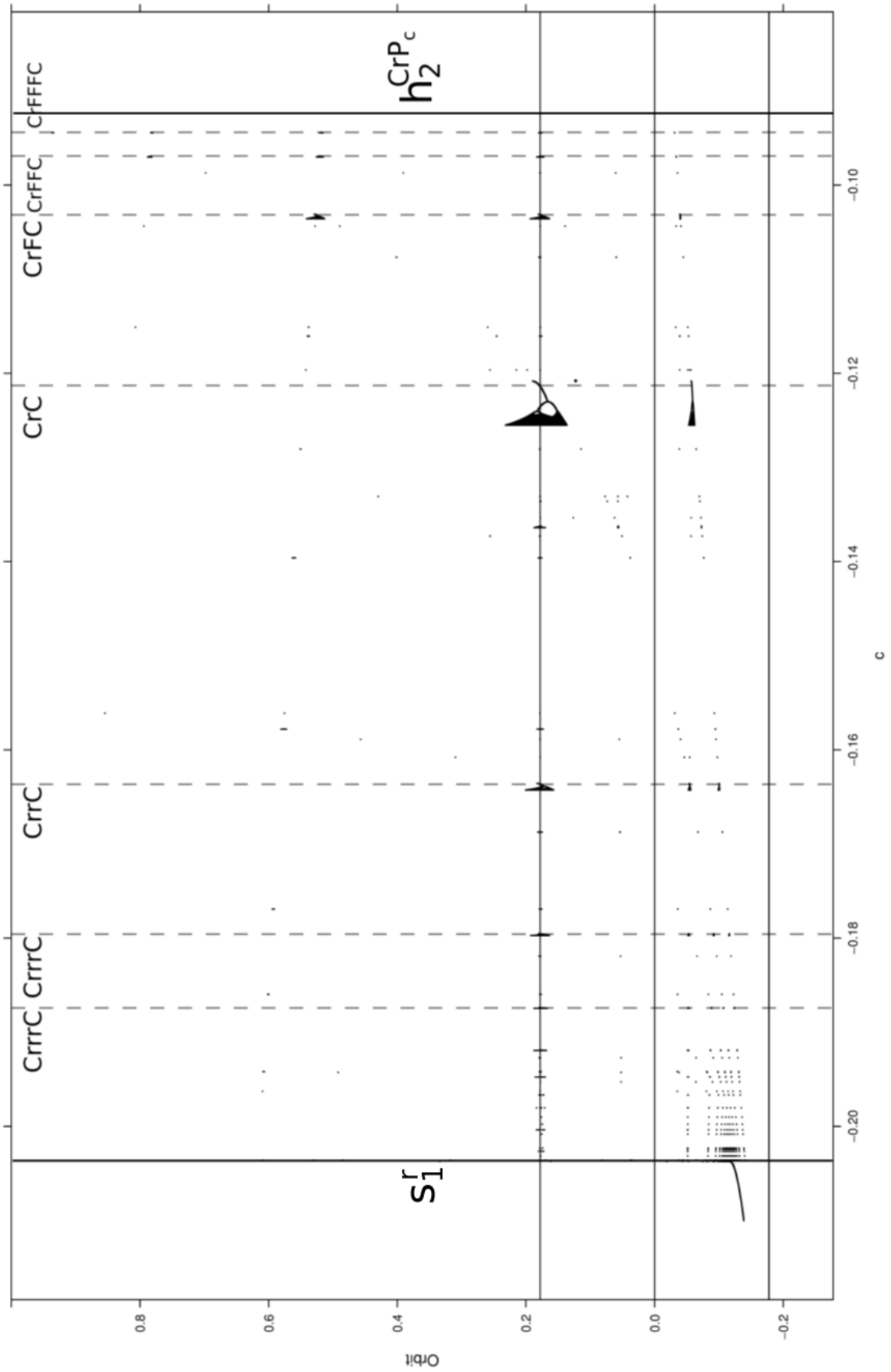

Fig. 3.8: A high quality orbit diagram with several p_n values and their codings indicated

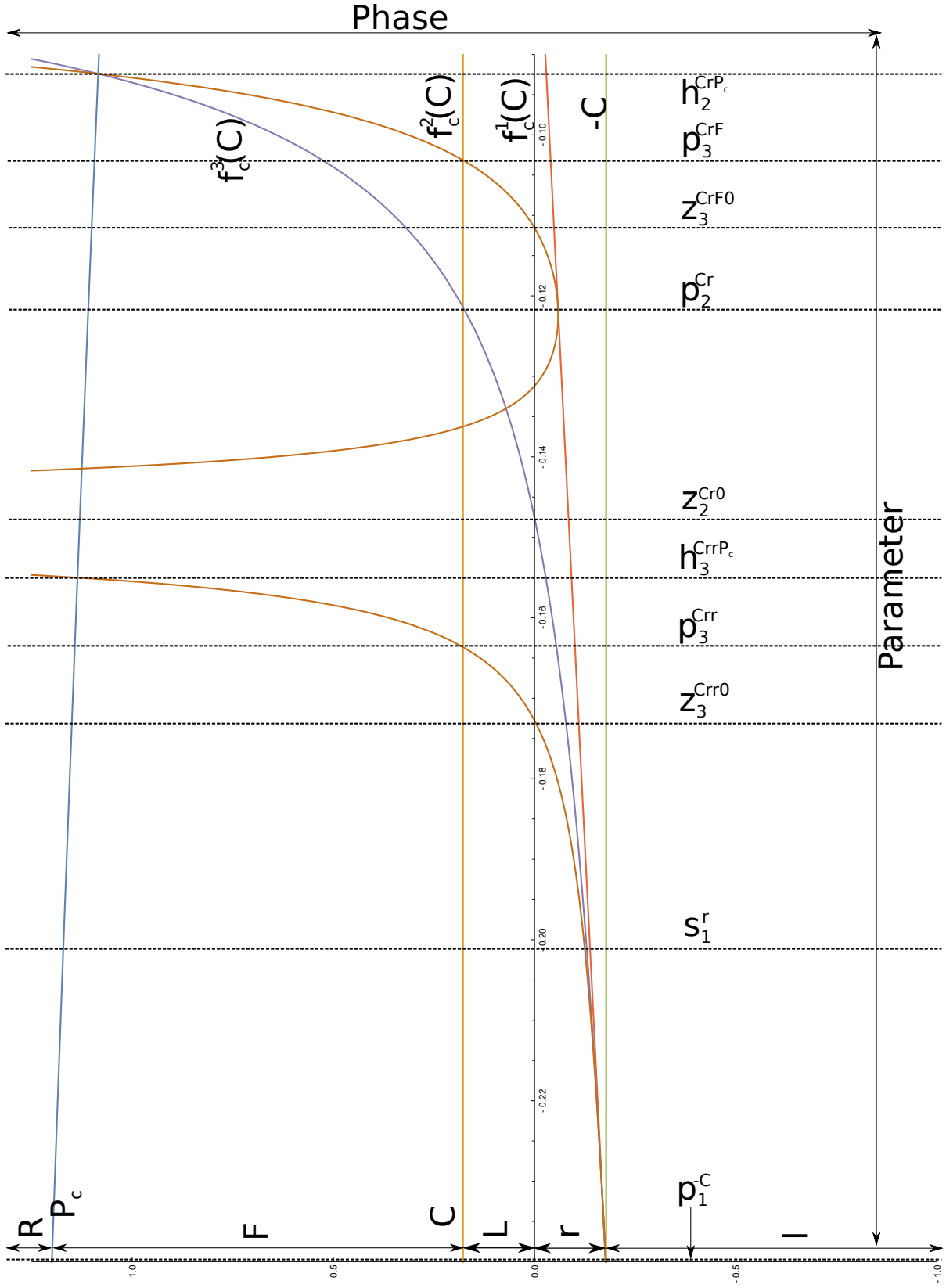

Fig. 3.9: A plot of $f_c^1(C), f_c^2(C), f_c^3(C)$ in parameter×phase space with the "primary" parameters labeled for h_n, p_n, z_n

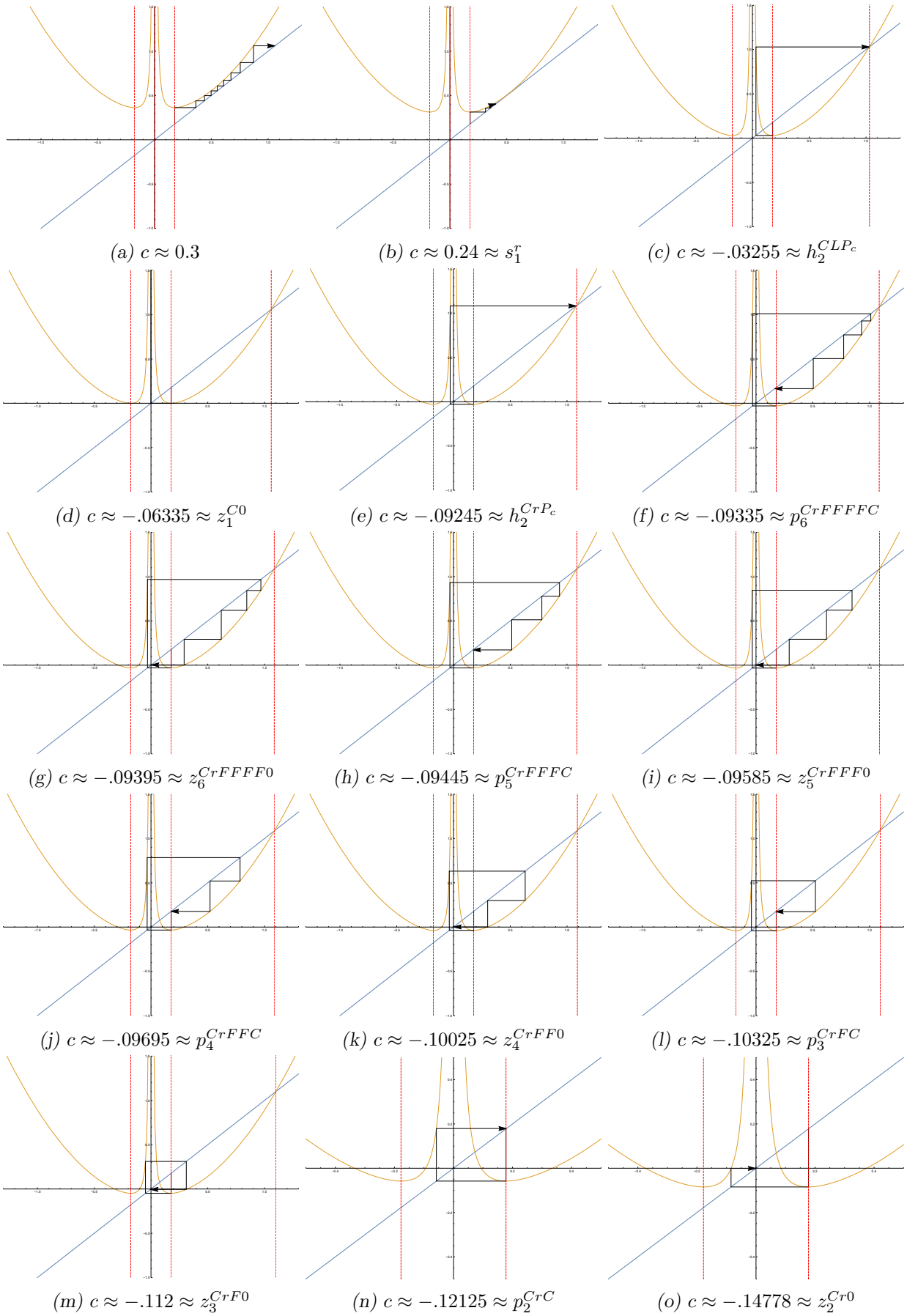

(a) $c \approx 0.3$ (b) $c \approx 0.24 \approx s_1^r$ (c) $c \approx -.03255 \approx h_2^{CLP_c}$

(d) $c \approx -.06335 \approx z_1^{C0}$ (e) $c \approx -.09245 \approx h_2^{CrP_c}$ (f) $c \approx -.09335 \approx p_6^{CrFFFFC}$

(g) $c \approx -.09395 \approx z_6^{CrFFFF0}$ (h) $c \approx -.09445 \approx p_5^{CrFFFC}$ (i) $c \approx -.09585 \approx z_5^{CrFFF0}$

(j) $c \approx -.09695 \approx p_4^{CrFFC}$ (k) $c \approx -.10025 \approx z_4^{CrFF0}$ (l) $c \approx -.10325 \approx p_3^{CrFC}$

(m) $c \approx -.112 \approx z_3^{CrF0}$ (n) $c \approx -.12125 \approx p_2^{CrC}$ (o) $c \approx -.14778 \approx z_2^{Cr0}$

Fig. 3.10: Graphical iteration showing the accumulation of periodic, prefixed, and prezero orbits as c approaches p_1^{-C} (depicted in 3.11 (k)) from the right and the accumulation of periodic, and prezero orbits as c approaches $h_2^{CrP_c}$ (depicted in 3.10 (e)) from the left

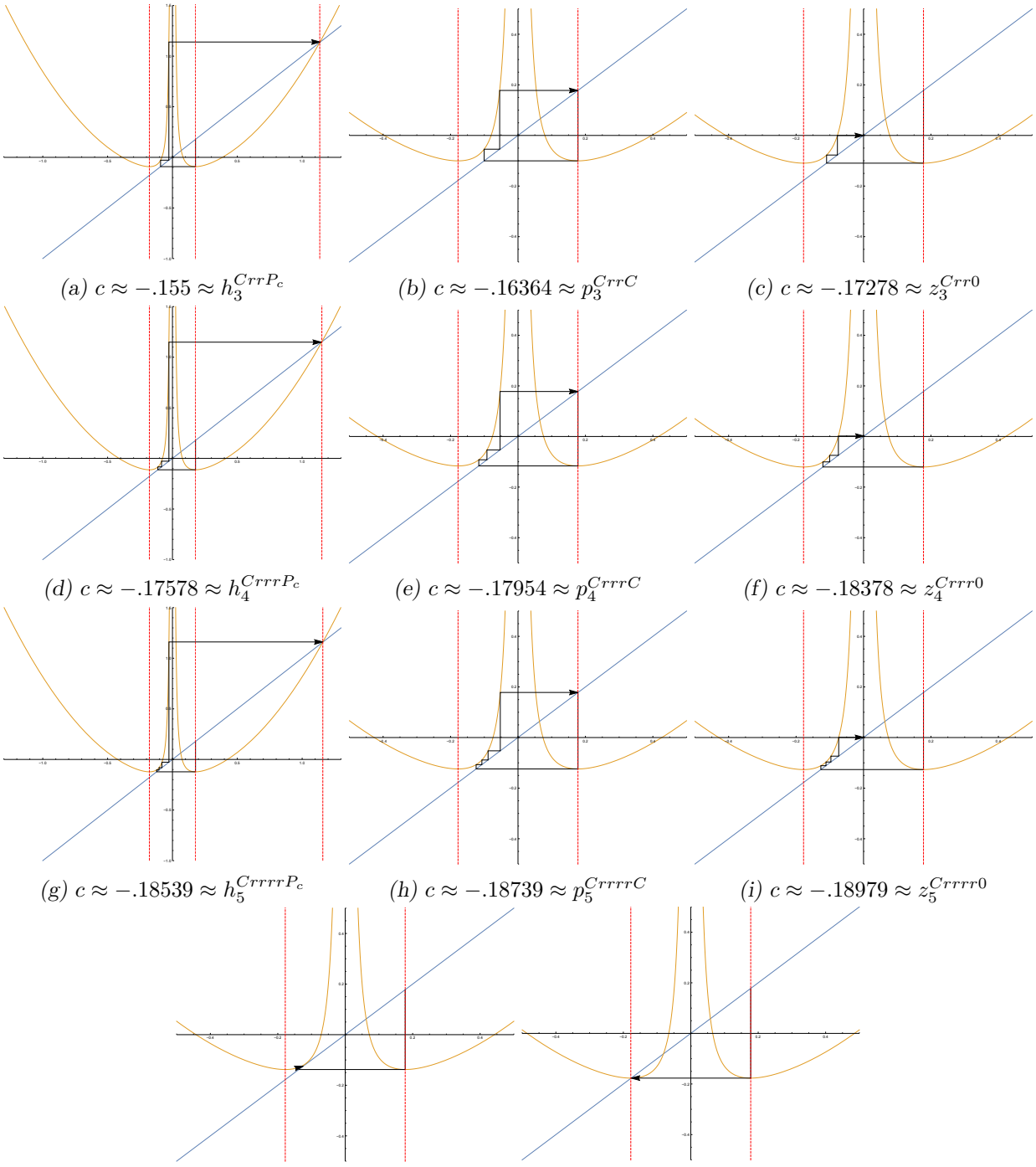

(a) $c \approx -.155 \approx h_3^{CrrP_c}$ (b) $c \approx -.16364 \approx p_3^{CrrC}$ (c) $c \approx -.17278 \approx z_3^{Crr0}$

(d) $c \approx -.17578 \approx h_4^{CrrrP_c}$ (e) $c \approx -.17954 \approx p_4^{CrrrC}$ (f) $c \approx -.18378 \approx z_4^{Crrr0}$

(g) $c \approx -.18539 \approx h_5^{CrrrrP_c}$ (h) $c \approx -.18739 \approx p_5^{CrrrrC}$ (i) $c \approx -.18979 \approx z_5^{Crrrr0}$

(j) $c \approx -.201 \approx s_1^l$ (k) $c \approx -.24 \approx p_1^{-C}$

Fig. 3.11: Graphical iteration showing the accumulation of periodic, prefixed, and prezero orbits as c approaches p_1^{-C} (depicted in 3.11 (k)) from the right and the accumulation of periodic, and prezero orbits as c approaches $h_2^{CrP_c}$ (depicted in 3.10 (e)) from the left (continued)

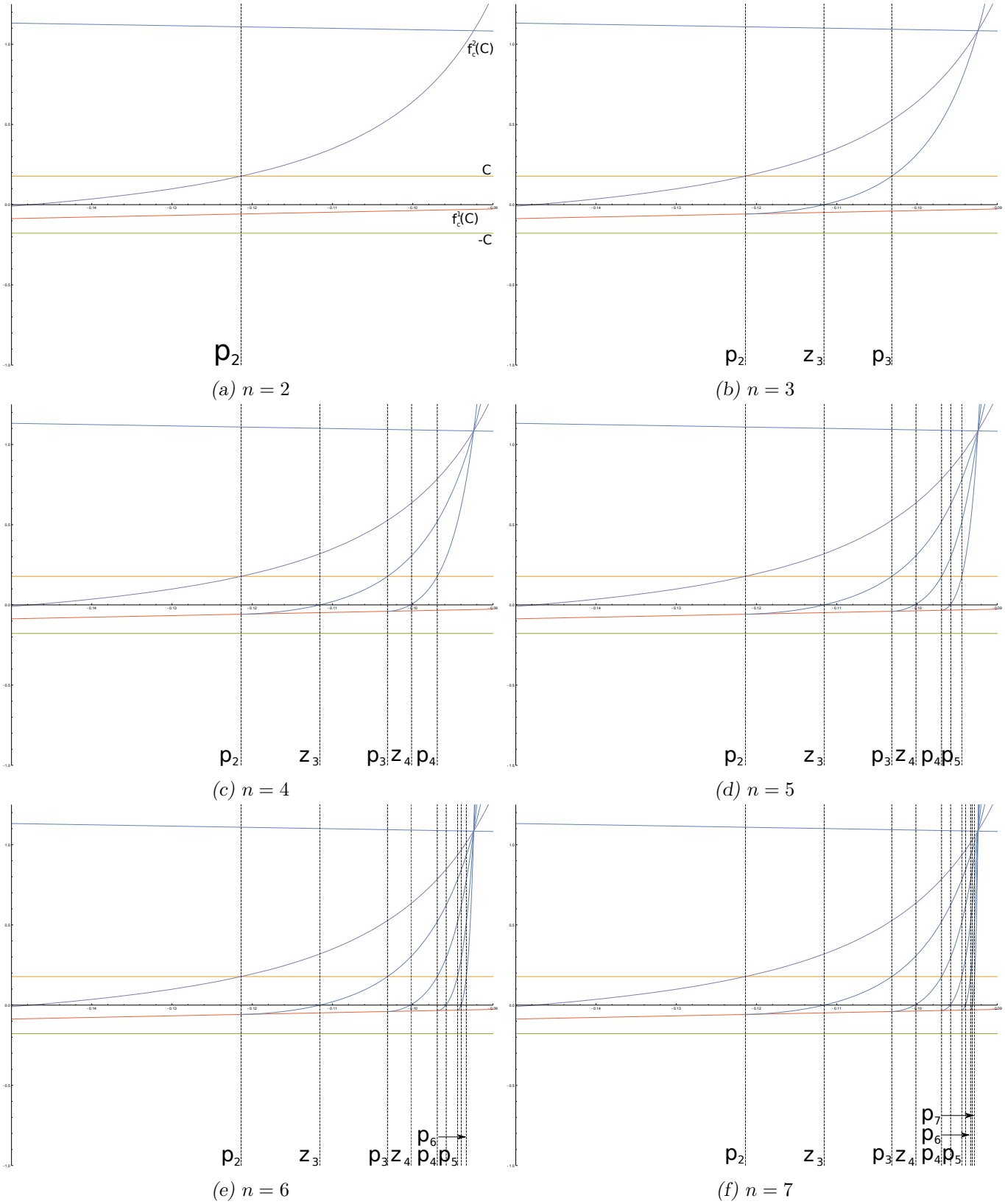

(a) $n = 2$ (b) $n = 3$ (c) $n = 4$ (d) $n = 5$ (e) $n = 6$ (f) $n = 7$

Fig. 3.12: Plots of various iterates of $f_c(C)$ as a function of c depicting the accumulation of prezero and periodic parameter values as we approach $h_2^{CrP_c}$ from the left. Note that for $n > 4$ the z_n values are marked but not labeled. Also observe that each $f_c^i(C)$ is only plotted on the interval $(p_{i-1}, h_2^{CrP_c})$ in order to highlight specific behaviors

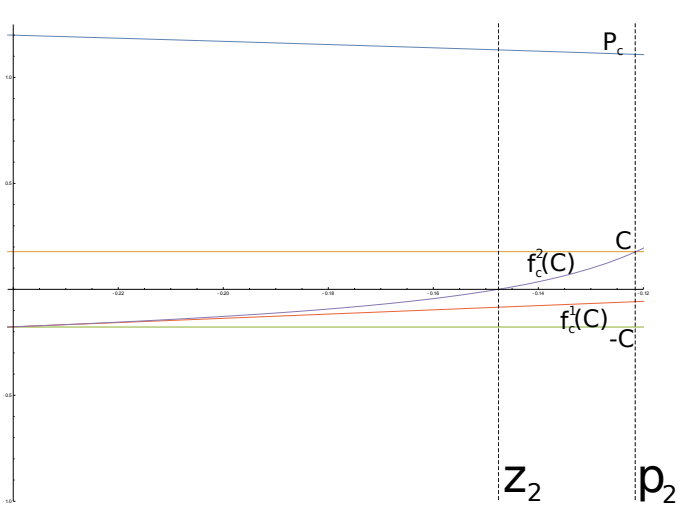

(a) First two iterates of $f_c(C)$ along with the parameter value of $f_c^2(C)$'s prezero orbit

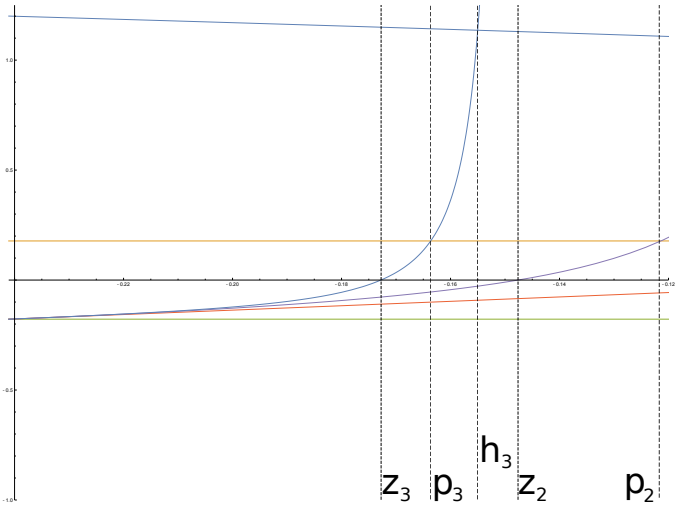

(b) Third iterate of $f_c(C)$ added along with the parameter value of its prezero orbit

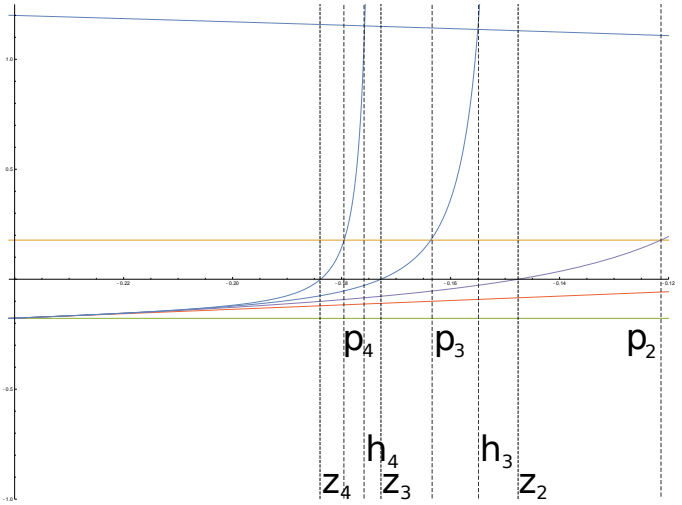

(c) Fourth iterate of $f_c(C)$ added along with the parameter value of its prezero orbit

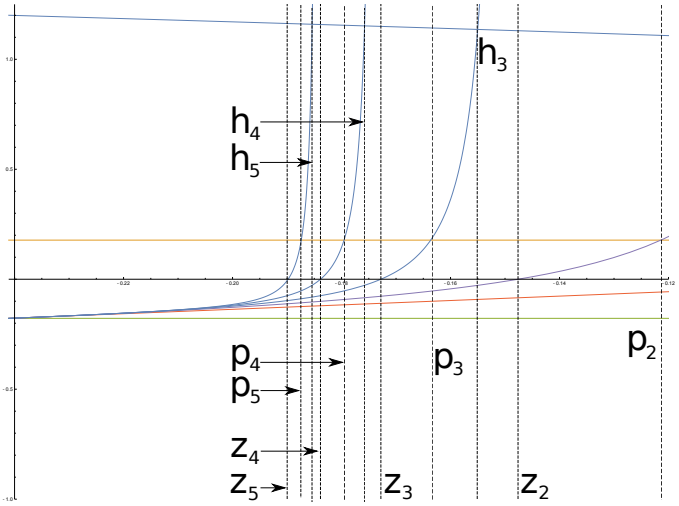

(d) Fifth iterate of $f_c(C)$ added along with the parameter value of its prezero orbit

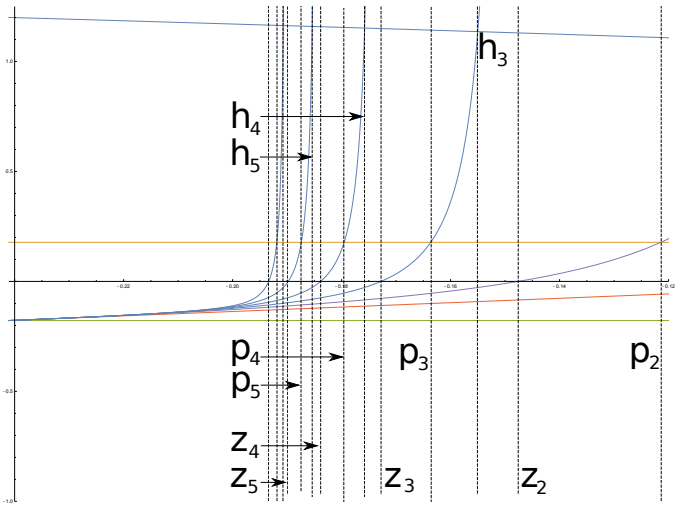

(e) Sixth iterate of $f_c(C)$ added along with the parameter value of its prezero orbit

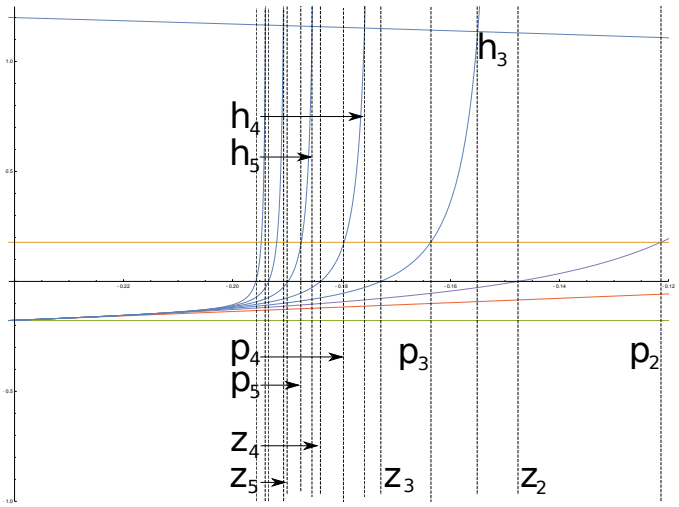

(f) Seventh iterate of $f_c(C)$ added along with the parameter value of its prezero orbit

Fig. 3.13: Plots of various iterates of $f_c(C)$ as a function of c depicting the accumulation of prezero, periodic, and prefixed parameter values as we approach s_1^l from the right. Note that for $n > 4$ the z_n and h_n values are marked but not labeled. Also observe that each $f_c^i(C)$ is only plotted on the interval (p_1^{-C}, z_{i-1}) in order to highlight specific behaviors

3.6 An Infinite Hierarchy of Prezero Points

Now that we have visually demonstrated the existence of these two "primary sequences" of parameter values, we will introduce some results which add an infinite hierarchy of complexity in between each parameter value in the aforementioned sequences. This result is best summarized by Proposition 4.4:

Proposition 4.4: *Suppose we have two distinct parameter values* $z_{n_1}^{C\alpha 0}, z_{n_2}^{C\beta 0} \in (p_1^{-C}, h_2^{CrP_c})$ *where* α *and* β *are coding sequences such that* $\alpha_i \neq \beta_i$ *for at least one* i*. Then there must be at least one other prezero parameter value* $z_{n_3}^{C\gamma 0}$ *on the interval int*$\{z_{n_1}^{C\alpha 0}, z_{n_2}^{C\beta 0}\}$ *such that* $\alpha_i \neq \gamma_i$ *and* $\beta_j \neq \gamma_j$ *for at least one* i *and one* j*.*

In this section we will briefly provide some discussion and figures which provide some intuition as to what this proposition means. First consider the plot of the first 3 iterates of the right hand critical point with respect to c as shown in the Figure 3.9. This plot is a useful visual guide because we can quickly see how the behavior of lower iterates affects the behavior of higher iterates. One of the most notable behaviors that can be observed is how some n^{th} iterate mapping to zero forces all higher iterates to be ∞, a fact easily proven as Lemma 4.7. Additionally, we note that for all $n > 2$, $f^n_{h_2^{CrP_c}}(C) = P_c$ and $f^n_{p_1^{-C}}(C) = -C$ as discussed in the introductory remarks. Thus at either end of this interval, all iterates are clamped to some specific value, regardless of the behavior in between.

To provide an example of what Proposition 4.4 is saying, we will provide a sample case from the proof of Proposition 4.2. Figure 3.14 shows the first case where we have some parameter z_3^{CrF0} to the left and some parameter z_4^{CrFL0} to the right. This proposition forces the existence of some other z_{n_1} between these two parameter values. Two satisfactory parameter values are labeled as z_5^{CrFLF0} and z_5^{CrFLL0}. Note that these values were found by looking at $f_c^4(C)$ which has a parameter value p_4^{CrFL} in between z_3^{CrF0} and z_4^{CrFL0}. Then we show in Chapter 4 that $f_c^1(C) < 0$ for $c \in (p_1^{-C}, h_2^{CrP_c})$, meaning that when we look at the fifth iterate at this parameter value we get:

$$f^5_{p_4^{CrFLC}}(C) = f_{p_4^{CrFLC}}\left(f^4_{p_4^{CrFLC}}(C)\right) = f_{p_4^{CrFLC}}(C) < 0$$

Thus we have a c value for which $f_c^5(C) < 0$ and two points where the fifth iterate must be ∞ (at z_3^{CrF0} and z_4^{CrFL0}) so in between there must be two points where the fifth iterate is 0, these being z_5^{CrFLF0} and z_5^{CrFLL0}.

In Chapter 4 we prove this for all n. An interesting implication of this theorem is that there are in fact an infinity of z_n values between any other $z_{n_1}, z_{n_2} \in (p_1^{-C}, h_2^{CrP_c})$ which additionally gives an infinity of h_n

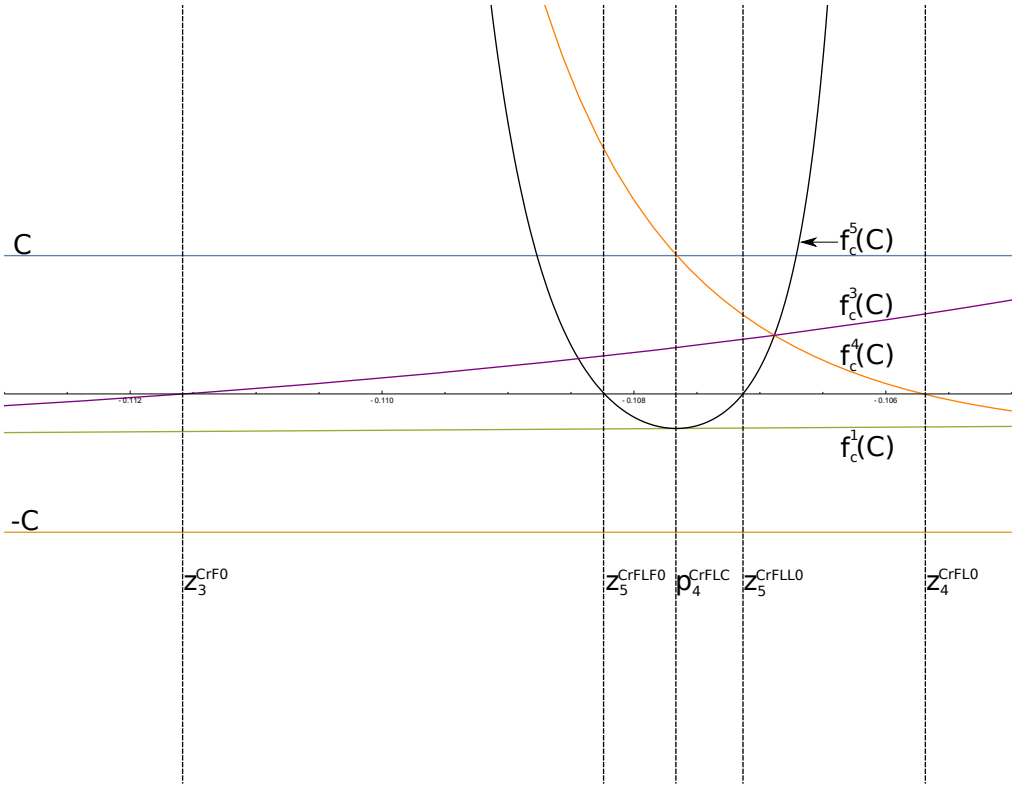

Fig. 3.14: Plot of $f_c(C), f_c^3(C), f_c^4(C)$ and part of $f_c^5(C)$ showing the existance of two prezero parameter values z_5^{CrFLF0} and z_5^{CrFLL0} between the outer two prezero parameter values z_3^{CrF0} and z_4^{CrFL0}

and p_n values as well. Thus the primary sequences we discussed in the previous section are just the first level of critical point behavior, giving rise to the infinite hierarchy that Proposition 4.4 fills in.

4. PROOF OF RESULTS

4.1 Accumulation of Special Parameter Values on Homoclinic Parameter Values

In this section we will discuss the interesting behavior as the system admits a homoclinic point as defined below.

Definition 4.1: Local Unstable Set[2]

Let $f(p) = p,\ |f'(p)| > 1$ such that p is a repelling fixed point. Then there must be an open interval about p on which f is one-to-one and satisfies the the expansion property $|f(x) - p| > |x - p|$. We define the local unstable set at p to be the maximal such open interval about p. We denote this set by $W^u_{loc}(p)$.

Definition 4.2: Homoclinic Point[2]

Let $f(p) = p$ and $f'(p) > 1$. A point q is called homoclinic to p if $q \in W^u_{loc}(p)$ and there exists $n > 0$ such that $f^n(q) = p$. The point q is heteroclinic if $q \in W^u_{loc}(p)$ and there exists $n > 0$ such that $f^n(q)$ lies on a different periodic orbit

The Figure 4.1 shows a parameter value for which the critical point is homoclinic to the right hand fixed point (depicted under graphical iteration). A more intuitive way of thinking about homoclinic points is that if a point q is homoclinic to p then q approaches p under forward and backward iteration.

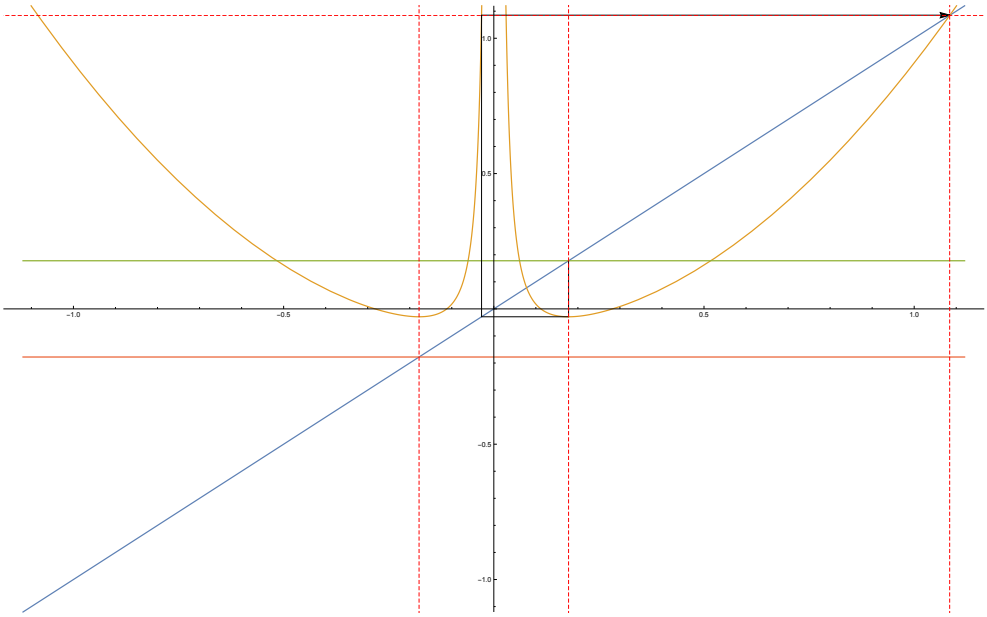

Fig. 4.1: Graphical iteration showing the "primary" homoclinic point of f at the parameter value $h_2^{CrP_c} \approx -0.092395$

One requirement common to most of the subsequent arguments is that we are working with a continuous map, something that f_c currently is not, given the discontinuity at zero. The following propositions allay these concerns by shifting our system to the two-point compactification of the reals, over which $f_c(x)$ is continuous.

Proposition 4.1:

The family of maps $f_c(x) = x^2 + c + \frac{.001}{x^2}$ is continuous with respect to x and c under the two point compactification of the reals.

Proof:

Consider $f : \mathbb{R} \to \mathbb{R}$ such that $f(x) = x^2 + c + \frac{.001}{x^2}$. Now let $\widetilde{\mathbb{R}} = \mathbb{R} \cup \{-\infty, \infty\}$ and consider $\widetilde{f}$ such that $\widetilde{f} : \widetilde{\mathbb{R}} \to \widetilde{\mathbb{R}}$ where f and $\widetilde{f}$ are equal at all points equal except $\widetilde{f}(-\infty) = \infty$, $\widetilde{f}(0) = \infty$, and $\widetilde{f}(\infty) = \infty$. Additionally consider the map $h(x) = \left(\frac{2}{\pi}\right)\arctan(x)$ where $h : \mathbb{R} \to (-1, 1)$ and the map $\widetilde{h} : \widetilde{\mathbb{R}} \to [-1, 1]$ where h and $\widetilde{h}$ are at all points equal except $\widetilde{h}(-\infty) = -1$ and $\widetilde{h}(\infty) = 1$. Now consider the following

conjugacy where $\widetilde{g_c} = \widetilde{h} \circ \widetilde{f_c} \circ \widetilde{h}^{-1}$:

$$\begin{array}{ccc} \widetilde{\mathbb{R}} & \xrightarrow{\widetilde{f_c}} & \widetilde{\mathbb{R}} \\ \downarrow{\scriptstyle \widetilde{h}} & & \downarrow{\scriptstyle \widetilde{h}} \\ [-1,1] & \xrightarrow{\widetilde{g_c}} & [-1,1] \end{array}$$

Plotting $\widetilde{g_c}$ we get the image in Figure 4.2. We can see that the function $\widetilde{g_c}(x)$ is clearly continuous in this extended space so we can conclude that $\widetilde{f_c}(x)$ is conjugate to a continuous map on the interval $[-1, 1]$ and consequently is itself continuous.

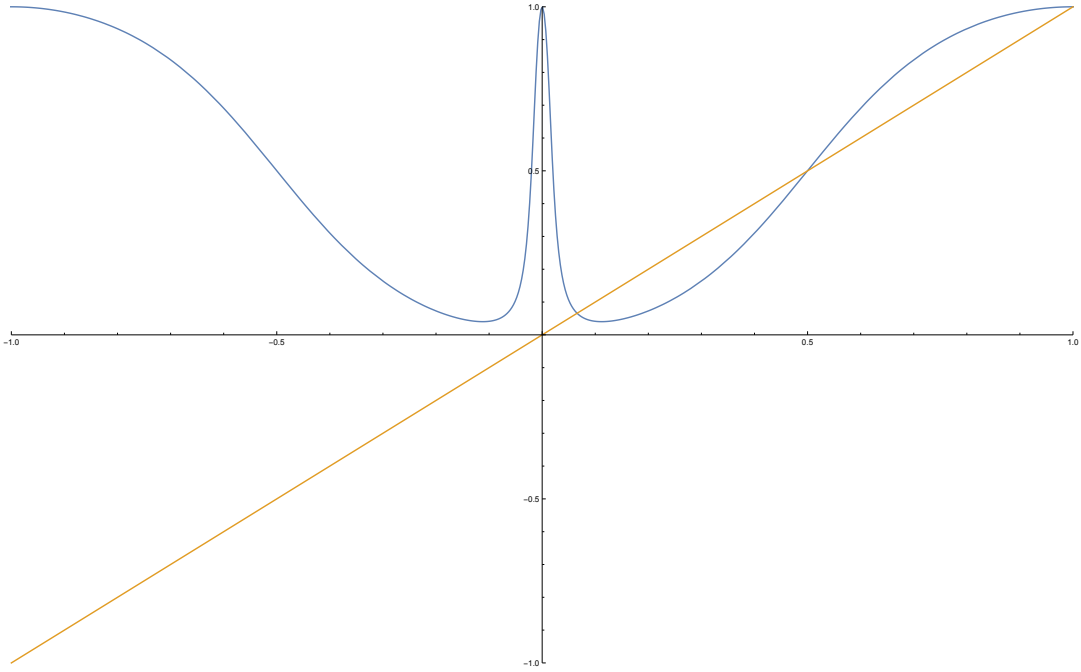

Fig. 4.2: The continuous function $\widetilde{g_c} : [-1, 1] \to [-1, 1]$ for $c = 0$ along with the reference line $y = x$

□

Thus in our extended space, we no longer need to worry about the discontinuity at 0. **For the remainder of the chapter, relabel $\widetilde{f}$ as f such that $f : \widetilde{\mathbb{R}} \to \widetilde{\mathbb{R}}$.** Additionally, we know that the composition of continuous maps is continuous so for all n, $f_c^n(x)$ is continuous with respect to x and c.

Before proceeding further, we must develop a description of how higher iterates change with respect to x

and c. First note that

$$\frac{\partial f_c(x)}{\partial x} = \frac{\partial}{\partial x}\left(x^2 + c + \frac{.001}{x^2}\right) = 2x - \frac{.002}{x^3}$$
$$\frac{\partial f_c(x)}{\partial c} = \frac{\partial}{\partial c}\left(x^2 + c + \frac{.001}{x^2}\right) = 1$$

For simplicity, we will denote the first function as $f'(x) = 2x - \frac{.002}{x^3}$. Note that since $f'(x)$ has an odd degree polynomial singularity, we do not have a continuous derivative under the aforementioned compactification. Now that we have obtained our derivative with respect to x and c, we can easily expand this to the derivative of the n^{th} iterate of $f_c(x)$ by using the chain rule. For now we rewrite our function such that $f_c(x) = f(x, c)$ where we are iterating under the following function composition:

$$f^n(x,c) = f^{n-1}(f(x,c),x) = f^{n-2}(f(f(x,c),c),c) = \cdots = \underbrace{f(f(f(\cdots,c),c),c)}_{n-1 \text{ times}}$$

Now let $z = f^n(x,c) = f\left(f^{n-1}(x,c), c\right) = f(v,c)$ where $v = f^{n-1}(x,c)$. Then we see that the derivative of the n^{th} iterate with respect to x is given by:

$$\begin{aligned}
\frac{\partial z}{\partial x} &= \frac{\partial z}{\partial v}\frac{\partial v}{\partial x} + \frac{\partial z}{\partial c}\frac{\partial c}{\partial x} \\
&= \left(\frac{\partial}{\partial v}\left(v^2 + c + \frac{.001}{v^2}\right)\right)\frac{\partial f^{n-1}(x,c)}{\partial x} + \left(\frac{\partial}{\partial c}\left(v^2 + c + \frac{.001}{v^2}\right)\right)\left(\frac{\partial}{\partial x}\ c\right) \\
&= \left(2v - \frac{.002}{v^3}\right)\frac{\partial f^{n-1}(x,c)}{\partial x} + (1)\cdot\left(\frac{\partial}{\partial x}\ c\right) \\
&= \left(f'\left(f^{n-1}(x,c)\right)\right)\frac{\partial f^{n-1}(x,c)}{\partial x} + \cancelto{0}{\left(\frac{\partial}{\partial x}\ c\right)} \\
&= f'\left(f^{n-1}(x,c)\right)\frac{\partial f^{n-1}(x,c)}{\partial x}
\end{aligned}$$

Then continuing this pattern for $\frac{\partial f^{n-1}}{\partial x}$ we get the following formula for the derivative of the n^{th} iterate with respect to x:

$$\frac{\partial f^n(x,c)}{\partial x} = \prod_{i=1}^{n-1} f'(f^i(x,c))$$

In a similar manner, we can compute the derivative of the n^{th} iterate with respect to c as follows:

$$\begin{aligned}
\frac{\partial z}{\partial c} &= \frac{\partial z}{\partial v}\frac{\partial v}{\partial c} + \frac{\partial z}{\partial c}\frac{\partial c}{\partial c} \\
&= \left(\frac{\partial}{\partial v}\left(v^2 + c + \frac{.001}{v^2}\right)\right)\frac{\partial f^{n-1}(x,c)}{\partial c} + \left(\frac{\partial}{\partial c}\left(v^2 + c + \frac{.001}{v^2}\right)\right)\left(\frac{\partial}{\partial c}\ c\right) \\
&= \left(2v - \frac{.002}{v^3}\right)\frac{\partial f^{n-1}(x,c)}{\partial c} + (1)\cdot\left(\frac{\partial}{\partial c}\ c\right) \\
&= \left(f'\left(f^{n-1}(x,c)\right)\right)\frac{\partial f^{n-1}(x,c)}{\partial c} + \cancel{\left(\frac{\partial}{\partial c}\ c\right)}^{1} \\
&= f'\left(f^{n-1}(x,c)\right)\frac{\partial f^{n-1}(x,c)}{\partial c} + 1
\end{aligned}$$

then continuing this pattern for $\frac{\partial f^{n-1}}{\partial c}$ we get the slightly more complicated equation:

$$\begin{aligned}
\frac{\partial f^n(x,c)}{\partial x} &= f'\left(f^{n-1}(x,c)\right)\frac{\partial f^{n-1}(x,c)}{\partial c} + 1 \\
&= f'\left(f^{n-1}(x,c)\right)\left(f'\left(f^{n-2}(x,c)\right)\frac{\partial f^{n-2}(x,c)}{\partial c} + 1\right) + 1 \\
&= \underbrace{f'\left(f^{n-1}(x,c)\right)\left(f'\left(f^{n-2}(x,c)\right)\left(f'\left(f^{n-3}(x,c)\right)(\cdots) + 1\right) + 1\right)}_{n-1 \text{ times}} + 1 \\
&= f'\left(f^{n-1}(x,c)\right)f'\left(f^{n-2}(x,c)\right)\cdots f'\left(f^{1}(x,c)\right) + f'\left(f^{n-1}(x,c)\right)f'\left(f^{n-2}(x,c)\right)\cdots f'\left(f^{2}(x,c)\right) + \\
&\cdots + f'\left(f^{n-1}(x,c)\right) + 1 \\
&= \sum_{i=0}^{n-1}\left(\prod_{j=0}^{i} f'\left(f^{n-j-1}(x,c)\right)\right) + 1
\end{aligned}$$

We will now use the derivatives computed above in the following lemmas and propositions. We first consider the periodic point accumulation towards the right hand fixed point at the parameter value $h_2^{CrP_c}$.

Lemma 4.1:

Let p_n and z_n be the special parameter values defined in Chapter 3. Then as $c \to h_2^{CrP_c}$ from the left, we will have some sequence of parameter values p_n and z_n for $n \geq 2$ such that

$$z_n < p_n < z_{n+1} < p_{n+1} < \cdots < h_2^{CrP_c}$$

Proof:

See Figure 3.12 for a useful visualization of the following argument. We will prove the original statement by induction on n:

Base Case: We can solve for $f_c^2(C) = 0$, $f_c^2(C) = C$ and $f_c^3(C) = 0$, $f_c^3(C) = C$ and doing so we find a satisfactory sequence of parameter values such that:

$$z_2 = -.147612, p_2 = -.121386, z_3 = -.111571, p_3 = -.103143 \Rightarrow z_2 < p_2 < z_3 < p_3 < h_2^{CrP_c}$$

Thus we have established a satisfactory base case.

Induction Step: Suppose that for all $n' \leq n$ there exists $z_{n'} < p_{n'} < z_{n'+1} < p_{n'+1} < h_2^{CrP_c}$. Now consider the $(n+1)^{th}$ case, we know that there exists $z_n < p_n < h_2^{CrP_c}$ where, by definition, $f_{z_n}^n(C) = 0$ and $f_{p_n}^n(C) = C$. Then by Lemma 4.7 we see that $f_{p_n}^{n+1}(C) = f_{p_n}^1(C) < 0$ and since $f_{h_2^{CrP_c}}^{n+1}(C) = P_c > C > 0$, we know by the I.V.T. there must exist some parameter values $z_{n+1}, p_{n+1} < h_2^{CrP_c}$ such that $f_{z_{n+1}}^{n+1}(C) = 0$ and $f_{p_{n+1}}^{n+1}(C) = C$ where $z_{n+1} < p_{n+1}$ (because $0 < C$).

Thus the n^{th} case implies the $(n+1)^{th}$ case so we can conclude that the statement holds for all n. □

Lemma 4.2:

Suppose there exists some parameter $p_n \in (p_1^{-C}, h_2^{CrP_c})$ where the orbit of C has the coding $CrF^{n-2}C$. Then $f_c^n(C) \in F$ for $c \in (p_n, h_2^{CrP_c})$.

Proof:

First note that all p_n parameter values are assumed to have the superscript $CrF^{n-2}C$. We will prove this statement by induction on n:

Base Case: We can solve $f_{p_2}^2(C) = C$ to find $p_2 \approx -.121386$ which, since $n = 2$, has coding $CrF^{n-2}C = CrF^{2-2}C = CrC$. Then we can compute $\dfrac{\partial f_c^2(C)}{\partial c} = f'(f_c(C))) + 1$ and since $f_c(C) \in r$ for $c \in (p_1^{-C}, h_2^{CrP_c})$ and r is an increasing branch, $f_c^2(C)$ has positive slope for $c \in (p_2, h_2^{CrP_c})$.

Thus we know that $f_c^2(C)$ is strictly increasing on $(p_2, h_2^{CrP_c})$ and since $f_{p_2}^2(C) = C$, $f_{h_2^{CrP_c}}^2(C) = P_c$, we can conclude that $f_c^2(C) \in (C, P_c) = F$ for $c \in (p_2, h_2^{CrP_c})$.

Induction Step: Suppose that for all $n' \leq n$, if there exists a periodic orbit with coding $CrF^{n'-2}C$ at $p_{n'}$, then $f_c^{n'}(C) \in F$ for $c \in (p_{n'}, h_2^{CrP_c})$. Now consider the orbit $CrF^{(n+1)-2}C = CrF^{n-1}C$ at the parameter value p_{n+1}. We know that $f_c^n(C) \in F$ for $c \in (p_n, h_2^{CrP_c}) \supset (p_{n+1}, h_2^{CrP_c})$ (since $p_n < p_{n+1}$). Thus when we consider the derivative of $f_c^{n+1}(C)$ we have:

$$\frac{\partial f_c^{n+1}(C)}{\partial c} = \sum_{i=0}^{(n+1)-1} \left(\prod_{j=0}^{i} f'(x_{(n+1)-j-1}) \right) + 1 = \sum_{i=0}^{n} \left(\prod_{j=0}^{i} f'(x_{n-j}) \right) + 1$$

where $x_i = f_c^i(C)$. Thus we see that the derivative of $f_c^{n+1}(C)$ is entirely determined by sums of products

of $f'(x_i)$. However, the induction hypothesis forces all elements of this orbit to be in r or F such that $x_i \in r$ or $x_i \in F$. By definition of r and F, we know that the $f_c(x)$ is increasing on these intervals. Thus each $f'(x_i) > 0$ for $i > 0$ (and 0 otherwise) so we are left with the sum of the products of positive terms, which must also be positive. Therefore we have established that the slope of $f_c^{n+1}(C)$ is positive for $(p_n, h_2^{CrP_c}) \supset (p_{n+1}, h_2^{CrP_c})$. Finally, since it is known that $f_{p_{n+1}}^{n+1}(C) = C$, $f_{h_2^{CrP_c}}^{n+1}(C) = P_c$, and $f_c^{n+1}(C)$ is strictly increasing on the interval $(p_{n+1}, h_2^{CrP_c})$, we can conclude that $f_c^{n+1}(C) \in (C, P_c) = F$ for $c \in (p_{n+1}, h_2^{CrP_c})$.

Therefore the n^{th} case implies the $(n+1)^{th}$ case so we can conclude that if there exists some $p_n \in (p_1^{-C}, h_2^{CrP_c})$ where the orbit of $f_{p_n}(C)$ has the coding $CrF^{n-2}C$, then $f_c^n(C) \in F$ for $c \in (p_n, h_2^{CrP_c})$. □

Proposition 4.2:

On the interval $(p_1^{-C}, h_2^{CrP_c})$, there is an accumulation of parameter values p_n and z_n for any integer $n \geq 2$ where the critical orbit has coding $CrF^{n-2}C$ and $CrF^{n-2}0$ respectively. These parameter values have the ordering

$$z_n < p_n < z_{n+1} < p_{n+1} < \cdots < h_2^{CrP_c}$$

Proof:

First we assume that every z_n and p_n in the following proof will have the superscript $CrF^{n-2}0$ and $CrF^{n-2}C$ respectively. We will prove the statement by induction on the value n:

Base Case: Consider the base case where $n = 2$. We want a parameter value c such that $f_c^2(C) = C$. As we saw in Lemma 4.2, $p_2 \approx -.12138 \in (p_1^{-C}, h_2^{CrP_c})$ gives us a period two with coding $CrF^{2-2}C = CrC$, as required.

Induction Step: Assume that there exists some $z_{n'}$ and $p_{n'}$ for all $n' \leq n$ such that $z_{n'-1} < p_{n'-1} < z_{n'} < p_{n'} < h_2^{CrP_c}$ with coding $CrF^{n'-2}0$ and $CrF^{n-2}C$ respectively.

Then by Lemma 4.1 we know that there must exist z_{n+1}, p_{n+1} such that

$$z_n < p_n < z_{n+1} < p_{n+1} < h_2^{CrP_c}$$

Additionally since z_n and p_n have codings $CrF^{n-2}0$ and $CrF^{n-2}C$ respectively, we know by Lemma 4.2 that z_{n+1} and p_{n+1} must have coding $CrF^{(n+1)-2}0 = CrF^{n-1}0$ and $CrF^{(n+1)-2}C = CrF^{n-1}C$ respectively.

Thus the n^{th} case implies the $(n+1)^{th}$ case so we conclude that the statement holds for all n.

□

We will now look at the accumulation of significant parameter values as c approaches p_1^{-C}.

Lemma 4.3:

Let p_n and z_n be the special parameter values defined in Chapter 3. Then as $c \to p_1^{-C}$ from the right, we will have some sequence of parameter values p_n, z_n, h_n for $n \geq 2$ such that

$$p_1^{-C} < \cdots < z_{n+1} < p_{n+1} < h_{n+1} < z_n < p_n < h_n$$

Proof:

See Figure 3.13 for a useful visualization of the following argument. We will prove this statement by induction on n:

Base Case: We can solve for $f_c^2(C) = 0$, $f_c^2(C) = C$, $f_c^2(C) = P_c$ and $f_c^3(C) = 0$, $f_c^3(C) = C$, $f_c^3(C) = P_c$ and doing so we find a satisfactory sequence of parameter values such that:

$$z_2 \approx -.147612, p_2 \approx -.121386, h_2 \approx -.03255, z_3 \approx -.17278, p_3 \approx -.16364, h_3 \approx -.15542$$
$$\Rightarrow p_1^{-C} < z_3 < p_3 < h_3 < z_2 < p_2 < h_2$$

Thus we have established a satisfactory base case.

Induction Step: Suppose that for all $n' \leq n$ there exists $p_1^{-C} < z_{n'} < p_{n'} < h_{n'} < z_{n'-1} < p_{n'-1} < h_{n'-1}$. Now consider the $(n+1)^{th}$ case, we know that there exists $p_1^{-C} < z_n < p_n < h_n$ where, by definition, $f_{z_n}^n(C) = 0$, $f_{p_n}^n(C) = C$ and $f_{h_n}^n(C) = P_c$. Then by Lemma 4.7, we know that $f_{z_n}^{n+1}(C) = \infty$. Then since $f_{p_1^{-C}}^{n+1}(C) = -C$, the I.V.T. gives us that $f_c^{n+1}(C)$ must pass through P_c, C, and 0 in that order at least once as we go from z_n to p_1^{-C} (from right to left) on the interval (p_1^{-C}, z_n). Thus we can call these parameters h_{n+1}, p_{n+1}, and z_{n+1} such that

$$p_1^{-C} < z_{n+1} < p_{n+1} < h_{n+1} < z_n < p_n < h_n$$

Thus the n^{th} case implies the $(n+1)^{th}$ case so we can conclude that the statement holds for all n. □

Lemma 4.4:

Suppose there exists some parameter $z_n \in (p_1^{-C}, h_2^{CrP_c})$ where the orbit of C has the coding $Cr^{n-1}0$. Then $f_c^n(C) \in r$ for $c \in (p_1^{-C}, z_n)$.

Proof:

First note that all z_n parameter values are assumed to have the superscript $Cr^{n-1}0$. We will prove this statement by induction on n:

Base Case: We can solve $f_{z_2}^c(C) = 0$ to find $z_2 \approx -.147612$ with coding $Cr^{2-1}0 = Cr0$. Then we can compute $\dfrac{\partial f_c^2(C)}{\partial c} = f'(f_c(C))) + 1$ and since $f_c(C) \in r$ for $c \in (p_1^{-C}, h_2^{CrP_c})$ and r is an increasing branch, $f_c^2(C)$ has positive slope for $c \in (p_1^{-C}, z_2)$.

Thus we know that $f_c^2(C)$ is strictly increasing on (p_1^{-C}, z_2) and since $f_{z_2}^2(C) = 0$, $f_{p_1^{-C}}^2(C) = -C$, we can conclude that $f_c^2(C) \in (-C, 0) = r$ for $c \in (p_1^{-C}, z_2)$.

Induction Step: Suppose that for all $n' \leq n$, if there exists a prezero orbit with coding $Cr^{n'-1}0$ at $z_{n'}$, then $f_c^{n'}(C) \in r$ for $c \in (p_1^{-C}, z_{n'1})$. Now consider the orbit $Cr^{(n+1)-1}C = Cr^nC$ at the parameter value z_{n+1}. We know that $f_c^n(C) \in r$ for $c \in (p_1^{-C}, z_n) \supset (p_1^{-C}, z_{n+1})$ (since $z_n > z_{n+1}$). Thus when we consider the derivative of $f_c^{n+1}(C)$ we have:

$$\frac{\partial f_c^{n+1}(C)}{\partial c} = \sum_{i=0}^{(n+1)-1} \left(\prod_{j=0}^{i} f'(x_{(n+1)-j-1}) \right) + 1 = \sum_{i=0}^{n} \left(\prod_{j=0}^{i} f'(x_{n-j}) \right) + 1$$

where $x_i = f_c^i(C)$. Thus we see that the derivative of $f_c^{n+1}(C)$ is entirely determined by sums of products of $f'(x_i)$. However, the induction hypothesis forces all elements of this orbit to be in r such that $x_i \in r$. By definition of r, we know that the $f_c(x)$ is increasing on these intervals. Thus each $f'(x_i) > 0$ for $i > 0$ (and 0 otherwise) so we are left with the sum of the products of positive terms, which must also be positive. Therefore we have established that the slope of $f_c^{n+1}(C)$ is positive for $(p_1^{-C}, z_n) \supset (p_1^{-C}, z_{n+1})$. Finally, since it is known that $f_{z_{n+1}}^{n+1}(C) = 0$, $f_{p_1^{-C}}^{n+1}(C) = -C$, and $f_c^{n+1}(C)$ is strictly increasing on the interval (p_1^{-C}, z_n), we can conclude that $f_c^{n+1}(C) \in (-C, 0) = r$ for $c \in (p_1^{-C}, z_n)$.

Therefore the n^{th} case implies the $(n+1)^{th}$ case so we can conclude that the statement holds for all n. □

Proposition 4.3:

On the interval $(p_1^{-C}, h_2^{CrP_c})$, there is an accumulation of parameter values p_n, z_n, and h_n for any integer $n \geq 1$ where the critical orbit has coding $Cr^{n-1}C$, $Cr^{n-1}0$, and $Cr^{n-1}P_c$ respectively. These parameter values have the ordering

$$p_1^{-C} < \cdots < z_{n+1} < p_{n+1} < h_{n+1} < z_n < p_n < h_n$$

Proof:

First we assume that every z_n, p_n, and h_n in the following proof will have the superscript $Cr^{n-1}0$, $CrF^{n-2}C$,

and $CrF^{n-2}P_c$ respectively. We will prove the statement by induction on the value n:

Base Case: Consider the base case where $n = 2$. We want a parameter value c such that $f_c^2(C) = C$. As we saw in Lemma 4.2, $p_2 \approx -.12138 \in (p_1^{-C}, h_2^{CrP_c})$ gives us a period two with coding $Cr^{2-1}C = CrC$, as required. Since $f_c^2(C)$ is increasing on $(p_1^{-C}, h_2^{CrP_c})$, there exists unique parameter values z_n and p_n such that $f_{z_n}^2(C) = 0$ and $f_{h_n}^2(C) = P_c$ with coding $Cr0$ and CrP_c respectively. Additionally since $0 < C < P_c$, the ordering of these parameter values must be $z_n < p_n < P_c$. Thus we have the base case for $n = 2$.

Induction Step: Assume that there exists some $z_{n'}$, $p_{n'}$, and $h_{n'}$ for all $n' \leq n$ such that $p_1^{-C} < z_{n'} < p_{n'} < h_{n'} < z_{n'-1} < p_{n'-1} < h_{n'-1}$ with coding $Cr^{n'-1}0$, $Cr^{n'-1}C$, and $Cr^{n'-1}P_c$ respectively.

Then by Lemma 4.3 we know that there must exist $z_{n+1}, p_{n+1}, h_{n+1}$ such that

$$p_1^{-C} < z_{n+1} < p_{n+1} < h_{n+1} < z_n < p_n < h_n$$

Additionally since z_n, p_n, h_n have codings $Cr^{n-1}0, Cr^{n-1}C, Cr^{n-1}P_c$ respectively, we know by Lemma 4.2 that z_{n+1}, p_{n+1}, and h_{n+1} must have coding $Cr^{(n+1)-1}0 = CrF^n0$, $Cr^{(n+1)-1}C = CrF^nC$, and $CrF^{(n+1)-1}P_c = Cr^nP_c$ respectively (because $(p_1^{-C}, z_{n+1}) \subset (p_1^{-C}, p_{n+1}) \subset (p_1^{-C}, h_{n+1}) \subset (p_1^{-C}, z_n)$).

Thus the n^{th} case implies the $(n+1)^{th}$ case so we conclude that the statement holds for all n.

□

4.2 An Infinity of Prezero Parameter Values

We will begin this section with some preliminary propositions and lemmas which will be used to prove the key result given in Proposition 4.4.

Lemma 4.5:

The right hand fixed point P_c is always greater than 0, when it exists.

Proof:

It is clear that that parameter c simply translates our curve up and down and do not change the overall shape. Thus, as c decreases, is impossible for the right hand fixed point to ever be less than 0 because it is always on the right side of the singularity. Thus $P_c > 0$ $\forall c$. □

Lemma 4.6:

The first iterate of the critical point $f_c^1(C) < 0$ for $c \in (p_1^{-C}, h_2^{CrP_c})$.

Proof:

Computing we see that $f_c^1(C) = (.001)^{\frac{1}{4}} + c + \frac{.001}{(.001)^{\frac{1}{4}}} = 0.0632456 + c$. Then since this function has slope 1 with respect to c, $f_{-.0632456}(C) = 0$, and $h_2^{CrP_c} < -.0632456$, it is clear that $f_c^1(C) < 0$ for $c \in (p_1^{-C}, h_2^{CrP_c})$. □

Lemma 4.7:

Suppose that $f_{z_n}^n(C) = 0$. Then $f_{z_n}^m(C) = \infty \ \forall m > n$.

Proof:

Suppose that $f_{z_n}^n(C) = 0$ and let $m > n$ such that $m - n = l > 0$. Then

$$f_{z_n}^m(C) = f_{z_n}^l(f_{z_n}^n(C)) = f_{z_n}^l(0) = f_{z_n}^{l-1}\left(0^2 + c + \frac{.001}{0^2}\right) = f_{z_n}^{l-1}(\infty) = \infty$$

Thus all higher iterates are mapped to ∞ as required. □

Lemma 4.8:

Suppose that $f_{c_1}^n(C) \leq 0$ and $f_{c_2}^n(C) = \infty$. Then for some $z_n, p_n, h_n \in int\{c_1, c_2\}$, $f_{z_n}^n(C) = 0$, $f_{p_n}^n(C) = C$, $f_{h_n}^n(C) = P_c$.

Proof: We know that f is continuous with respect to c and that $C > 0$, $P_c > 0$ for all c. Then by the I.V.T., $f_c^n(C)$ must cross 0, C, and P_c as it ranges to ∞ so there must be some $z_n, p_n, h_n \in \text{int}\{c_1, c_2\}$ such that $f_{z_n}^n(C) = 0$, $f_{p_n}^n(C) = C$, $f_{h_n}^n(C) = P_c$. □

Lemma 4.9:

Suppose there exists some prime period n critical orbit at the parameter p_n such that $f_{p_n}^n(C) = C$. Then $f_{p_n}^l(C) = f_{p_n}^k(C)$ where k and l are positive integers satisfying $k \equiv_n l$.

Proof:

Suppose that the critical orbit at the parameter value p_n is of prime period n and let $l \in \mathbb{N}$ be given such that $l \equiv_n k$ which is to say that there exists $m \in \mathbb{N}^+$ such that $l - m \cdot n = k > 0$. Thus it will suffice to show that $f_{p_n}^l(C) = f_{p_n}^{k+m\cdot n}(C) = f_{p_n}^k(C)$, we will do so by induction on m:

Base Case:

Let $m = 0$, then it is clear that $f_{p_n}^{k+0\cdot n}(C) = f_{p_n}^k(C)$.

Induction Step:

Suppose that $f_{p_n}^{k+m'\cdot n}(C) = f_{p_n}^{k}(C)$ for all $m' \leq m$. Then:

$$f_{p_n}^{k+(m+1)n}(C) = f_{p_n}^{k+m\cdot n}(f_{p_n}^{n}(C)) \tag{4.1}$$

$$= f_{p_n}^{k+m\cdot n}(C) \tag{4.2}$$

$$= f_{p_n}^{k}(C) \tag{4.3}$$

where line (4.2) is given by $f_{p_n}^{n}(C) = C$ (by assumption) and line (4.3) is implied by the induction hypothesis. Thus the m^{th} case implies $(m+1)^{th}$ case so we can conclude that the statement holds for all n. □

Lemma 4.10:

Suppose that $f_{p_m}^{n}(C) = C$ for $p_m \in (p_1^{-C}, h_2^{CrP_c})$. Then there is a critical period $m = \frac{n}{a}$ orbit for some divisor a of n at p_m.

Proof:

Since $f_{p_m}^{n}(C) = C$ we know that C is mapped to itself after n iterations. Thus p_m may yield a periodic orbit of length n or possibly some divisor of n (since this may not be the lowest i such that $f_{p_m}^{i}(C) = C$). Thus we say generally that there must be some divisor a of n such that there is a period $m = \frac{n}{a}$ critical orbit at p_m. □

Lemma 4.11:

Suppose that there exists some coding sequences α, β and some parameter values $z_n^{C\alpha 0}, z_n^{C\beta 0} \in (p_1^{-C}, h_2^{CrP_c})$ such that $f_{z_n^{C\alpha 0}}^{n}(C) = 0$ and $f_{z_n^{C\beta 0}}^{n}(C) = 0$ where $f_c^n(C) \neq \infty$ and $f_c^n(C) \neq 0$ for $c \in int\{z_n^{C\alpha 0}, z_n^{C\beta 0}\}$ and $\alpha_i \neq \beta_i$ for at least one i. Then for some $m \leq n$, there exists $p_m \in int\{z_n^{C\alpha 0}, z_n^{C\beta 0}\}$ such that $f_{p_m}^{m}(C) = C$.

Proof:

Let $z_n^{C\alpha 0}, z_n^{C\beta 0}$ be two parameter values which induce n^{th} order prezero points such that $\alpha_i \neq \beta_i$ for at least one i. Since $c \geq p_1^{-C}$, we know that no $\alpha_i = l$ or $\beta_i = l$ because no critical iterate can cross over to the l interval before p_1^{-C}. Additionally, no $\alpha_i = R$ or $\beta_i = R$ because otherwise all subsequent iterates would have the coding R. Thus for any $i \leq n-1$, $\alpha_i \in \{r, L, F\}$ and $\beta_i \in \{r, L, F\}$.

Now suppose some m^{th} code is different between the two sequences such that $\alpha_m \neq \beta_m$ which is to say that the m^{th} iterate changed its coding on the interval $\text{int}\{z_n^{C\alpha 0}, z_n^{C\beta 0}\}$ for $m \leq n-1$. By continuity, we could not have the transitions $r \leftrightarrow F$ or $r \leftrightarrow L$ because these would cause some code to be 0 for some

parameter in int$\{z_n^{C\alpha 0}, z_n^{C\beta 0}\}$, and since $m \leq n-1$, this would force $f_c^n(C) = \infty$, violating our assumption that $f_c^n(C) \neq \infty$ on the interval int$\{z_n^{C\alpha 0}, z_n^{C\beta 0}\}$.

Therefore the only possible coding transitions on the interval int$\{z_n^{C\alpha 0}, z_n^{C\beta 0}\}$ are $L \to F$ or $F \to L$. In either case, Table 3.1 gives us that the m^{th} iterate must have transitioned continuously from one interval to the other, forcing the existence of some $p_m \in$ int$\{z_n^{C\alpha 0}, z_n^{C\beta 0}\}$ where $f_{p_m}^m(C) = C$, as required. □

Thus with these lemmas in hand, we can prove this section's main result:

Proposition 4.4:

Suppose we have two distinct parameter values $z_{n_1}^{C\alpha 0}, z_{n_2}^{C\beta 0} \in (p_1^{-C}, h_2^{CrP_c})$ where α and β are coding sequences such that $\alpha_i \neq \beta_i$ for at least one i. Then there must be at least one other prezero parameter value $z_{n_3}^{C\gamma 0}$ on the interval int$\{z_{n_1}^{C\alpha 0}, z_{n_2}^{C\beta 0}\}$ such that $\alpha_i \neq \gamma_i$ and $\beta_j \neq \gamma_j$ for at least one i and one j.

Proof:

Consider the following 2 cases:

1. $\underline{n_1 \neq n_2}$

   Assume $n_1 \neq n_2$ and suppose without loss of generality that $n_1 < n_2$. Then by Lemma 4.7 we know that $f_{z_{n_1}^{C\alpha 0}}^{n_2}(C) = \infty$. Thus we are guaranteed by Lemma 4.8 that there exists some $p_{n_2} \in$ int$\{z_{n_1}^{C\alpha 0}, z_{n_2}^{C\beta 0}\}$ where $f_{p_{n_2}}^{n_2}(C) = C$. Then considering the $(n_2+1)^{th}$ iterate we see that:

$$f_{p_{n_2}}^{n_2+1}(C) = f_{p_{n_2}}(f_{p_{n_2}}^{n_2}(C)) = f_{p_{n_2}}(C) < 0 \text{ and } f_{z_{n_1}^{C\alpha 0}}^{n_2+1}(C) = \infty = f_{z_{n_2}^{C\beta 0}}^{n_2+1}(C)$$

   Thus $f_c^{n_2+1}(C)$ must have had a zero in each of the intervals int$\{z_{n_1}^{C\alpha 0}, p_{n_2}\}$ and int$\{p_{n_2}, z_{n_2}^{C\beta 0}\}$. Therefore we have exhibited two parameter values which yield prezero critical orbits on the interval int$\{z_{n_1}^{C\alpha 0}, z_{n_2}^{C\beta 0}\}$. Additionally, since $n_2+1 > n_2 > n_1$, choosing either of these parameter values would give a new prezero parameter value with a different coding than either $z_{n_1}^{C\alpha 0}$ or $z_{n_2}^{C\beta 0}$ (because they have different lengths) as required. We expect these parameter values themselves to have different codings as well, although this is not necessary for the proof.

2. $\underline{n_1 = n_2}$

   Now suppose that $n_1 = n_2 = n$. We will consider each the following subcases:

   (a) $\underline{f_c^n(C) \neq \infty \text{ for any } c \in \text{int}\{z_n^{C\alpha 0}, z_n^{C\beta 0}\}}$

Suppose that $f^n_{z_n^{C\alpha 0}}(C) = 0$ and $f^n_{z_n^{C\beta 0}}(C) = 0$ such that $f^n_c(C) \neq \infty$ for $c \in \text{int}\{z_n^{C\alpha 0}, z_n^{C\beta 0}\}$. Then by Lemma 4.11 we know that there must exist some $p_m \in \text{int}\{z_n^{C\alpha 0}, z_n^{C\beta 0}\}$ such that $f^m_{p_m}(C) = C$ for some $m < n$.

Select any l such that $l = n + (m-n)_m + 1$ and $l > n$. Since $l \equiv_m 1$, Lemma 4.9 tells us that $f^l_{p_m}(C) = f^1_{p_m}(C)$ which forces $f^l_{p_m}(C) < 0$. Then since $f^n_{z_n^{C\alpha 0}}(C) = 0 = f^n_{z_n^{C\beta 0}}(C)$, Lemma 4.7 gives us that $f^l_{z_n^{C\alpha 0}}(C) = \infty = f^l_{z_n^{C\beta 0}}(C)$.

Therefore $f^l_c(C)$ must have a prezero orbit in $\text{int}\{z_n^{C\alpha 0}, p_m\}$ and $\text{int}\{p_m, z_n^{C\beta 0}\}$, giving us two prezero critical orbits. Additionally, since $n+1 > n$, choosing either of these parameter values would give a new prezero parameter value with a different coding than either $z_n^{C\alpha 0}$ or $z_n^{C\beta 0}$ (because they have different lengths) as required. We expect these parameter values themselves to have different codings as well.

(b) $\underline{f^n_c(C) = \infty \text{ for some } c \in \text{int}\{z_n^{C\alpha 0}, z_n^{C\beta 0}\}}$

Suppose that $f^n_{z_n^{C\alpha 0}}(C) = 0$ and $f^n_{z_n^{C\beta 0}}(C) = 0$ such that $f^n_{z_m}(C) = \infty$ for some $z_m \in \text{int}\{z_n^{C\alpha 0}, z_n^{C\beta 0}\}$ and $m < n$. Then since $f^n_{z_m}(C) = \infty$, we know that $f^n_c(C)$ must cross the positive critical point at least once (since $C \in (0, \infty)$), call the parameter of this intersection p_n. Thus we have $f^n_{p_n}(C) = C$ which implies that $f^{n+1}_{p_n}(C) = f^1_{p_n}(C) < 0$. Thus since $f^{n+1}_{p_n}(C) < 0$ and $f^{n+1}_{z_n^{C\alpha 0}}(C) = \infty = f^{n+1}_{z_n^{C\beta 0}}$, $f^{n+1}_c(C)$ must go through 0 at least twice, giving us two pre-zero critical orbits. Additionally, since $n+1 > n$, choosing either of these parameter values would give a new prezero parameter value with a different coding than either $z_n^{C\alpha 0}$ or $z_n^{C\beta 0}$ (because they have different lengths) as required. We expect these parameter values themselves to have different codings as well.

□

Note that while the proof above is for prezero points, it can easily be shown that between any two prezero parameter values, of a different coding, there are superattracting and prefixed parameter values as well.

5. BACK TO $\mathbb{R}^2$

The bulk of the discussion thus far has focused on the one dimensional dynamics of the map $f_{c,\beta}$. The goal of this chapter is to briefly consider the implications of the one-dimensional results on the overall

two-dimensional system. The results from the previous chapters pertain to finding parameter values which correspond to certain dynamical behaviors: superattracting periodic (p_n), prezero (z_n), and homoclinic (h_n). It would be natural to look for corresponding features within the parameter space escape images of our family. We focus here on the parameter values which yield escaping critical orbits, namely the prezero parameter values, z_n.

Figure 5.1 shows a zoom of the parameter space escape image for the map $f_{c,.001} = z^2 + c + \frac{.001}{\bar{z}^2}$. On top of this escape image we have overlaid some of the z_n parameter values that are part of the sequence approaching s_1^r from the left. We can clearly see that along the x, or real, axis, there is a region of white corresponding to each of these parameter values. These white areas correspond to regions of escape, as we would expect: exactly along the real axis, the critical orbit is prezero which means that nearby points would also be drawn in toward zero and subsequently escape. In addition to the plotted z_n values, it is also clear that there are many, many more escape regions along the real axis. These regions are a consequence of Proposition 4.4 which provides the infinite levels of parameter values causing escaping orbits.

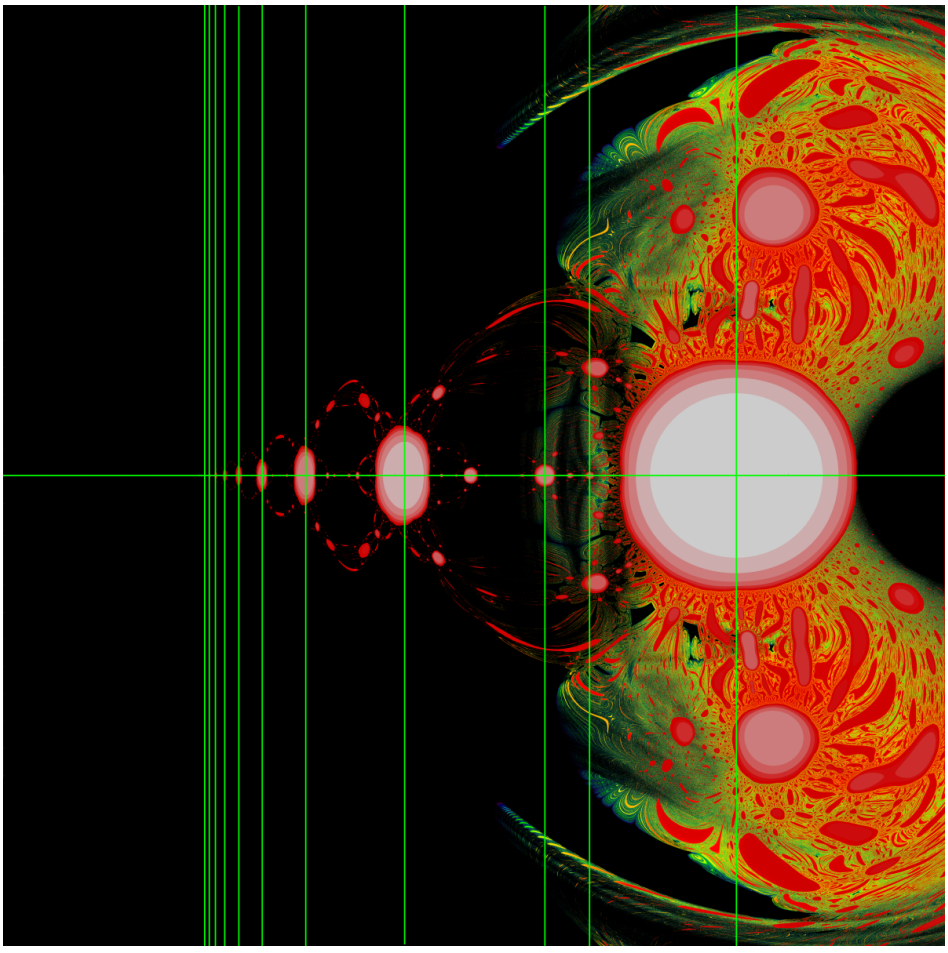

Fig. 5.1: Zoom of Figure 2.2b close to the real axis with the z_n parameter values labeled with vertical green lines

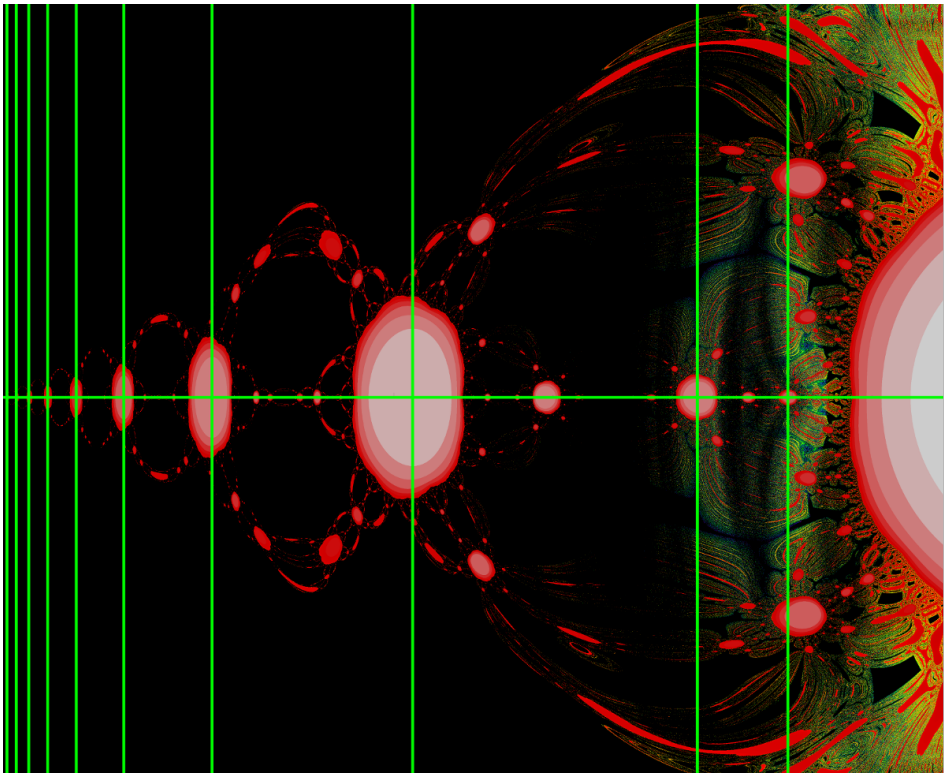

Fig. 5.2: A further zoom of Figure 5.1 showing the accumulation of the z_n parameter values

6. CONCLUSIONS AND FUTURE WORK

This paper has introduced several results pertaining to the behavior of the critical orbit of a very special subset of the rational maps of the plane. In the introduction we proposed a study of the larger two-dimensional, two parameter family $f_{c,\beta}$. While the results of this paper are not trivial, they largely pertain only to the real "spine" of this system where we held $\beta = .001$ and varied the complex parameter c, restricting c to be real. As such, there are many open questions that remain:

- This paper focused exclusively on the behavior of the critical orbit. While there are good reasons for doing so (see Schwarzian discussion in Section 3.1), a full description of the dynamics would require a discussion of the long term orbits of all points, not just the critical point. Thus the most natural future study would be to consider other orbits than the critical orbit.

- In addition to the parameter accumulations described thus far, there seems to be additional accumu-

lations for the real function. Looking at images like Figure 3.9 but with higher iterates, there seems to be a new accumulations of the z_n and p_n parameter values near every h_n parameter value (where f_c admits a critical homoclinic orbit). This is readily apparent by surveying the graphical iteration diagrams in Figures 3.10 and 3.11: every time there is a homclinic orbit, parameter values arbitrarily close to this value yield arbitrarily high order periodic and prezero orbits.

- We arbitrarily fixed the perturbation term β at .001. We know that for $\beta < 0$, the asymptote is directed toward $-\infty$, and consequently there are no critical points (making our technique irrelevant: there are no critical orbits to consider). However it would be interesting to see which ranges of β the described behavior holds and what other behaviors may arise as β varies.

- In order to introduce the continuity arguments in Chapter 4, we considered our map under a two-point compactification of the reals. When we plot the resulting function, it has a similar shape to a 4^{th} degree polynomial such as $x^4 - x^2$. While the maps are definitely very different, it would be interesting to see what structure they share.

- It would be interesting to see if there are any parallels to the h_n, p_n, and z_n accumulations in the complex plane. Looking at Figures 5.1 and 5.2, there seems to be patterns of escape regions in the real$\times$imaginary space which connect the explained escape regions along the real axis. Based on the complexity of the one-dimensional map, these two-dimensional structures would likely be very interesting to explore.

While this study focused on just the real part of a special family within this problem space, we were still able to uncover infinite levels of nontrivial behavior. It is this complexity, in addition to the new questions outlined above, which tells us 1) that there is a great amount of work to be done in order to understand all maps of the plane and 2) that these maps, even simplified special cases, can exhibit complex behavior which is worth studying.

WORKS CITED

[1] Brett Bozyck and Bruce Peckham. Nonholomorphic singular continuation: a case with radial symmetry. *International Journal of Bifurcation and Chaos*, 23(11), 2013.

[2] Robert L Devaney. *An introduction to chaotic dynamical systems.* Studies in Nonlinearity. Addison-Wesley, Menlo Park, California, Redwood City, CA, 1989.

[3] Robert L Devaney. *A First Course In Chaotic Dynamical Systems: Theory And Experiment.* Studies in Nonlinearity. Westview Press, New York, 1992.

[4] Antonio Garijo Sebastian M. Marotta Elizabeth D. Russell Paul Blanchard, Robert L. Devaney. *Rabbits, Basilicas, and Other Julia Sets Wrapped in Sierpinski Carpets.* Ak Peters Series. Taylor & Francis, 2009.